PERFORMANCE OF A COMPOSITE PALLADIUM MEMBRANE REACTOR FOR THE DEHYDROGENATION OF ETHYLBENZENE TO STYRENE

A Thesis

Presented to

the Faculty of the Department of Chemical and Biomolecular Engineering

University of Houston

In Partial Fulfillment

of the Requirements for the Degree

Master of Science

in Chemical Engineering

by

Ogochukwu Yvonne Enekwizu

May 2013

Acknowledgements

I'm grateful to God; I really couldn't have gotten to where I am now without trusting Him about everything.

Special thanks go to my advisor, Dr. Michael Harold, for guiding me on the research. I'm also grateful to him for his patience and faith in me when everything seemed to be going awry.

I'd also like to thank Carl Hill, without whom this project would not have been possible. He basically took me under his wing and patiently taught me how to use the gas chromatograph and assisted me in the construction of the entire experimental setup. His optimism was a strong factor that kept me going!

Special thanks go to Dr. Mai Ha and Dr. Sameer Israni who, regardless of distance, patiently and meticulously guided me through the workings in the lab. They taught me several experimental techniques, especially the synthesis of palladium membranes.

Many thanks to my beloved family: Dad and Mom, for their unwavering love and support; to my siblings Emeka, Gozie and Adaobi for constantly encouraging me. You guys are the best cheerleaders anyone could ask for.

A lot of thanks go to my friends: Sachi, Aseem and Tayebeh for their support and companionship in the lab, to the Bridges family especially Kristine for inspiration and comfort, to my friends at Mission 24 for constantly praying and believing in me, to Carmen and Prati, my fellow musketeers, and to friends back home who always sent their love and support.

PERFORMANCE OF A COMPOSITE PALLADIUM MEMBRANE REACTOR FOR THE DEHYDROGENATION OF ETHYLBENZENE TO STYRENE

An Abstract

of a

Thesis

Presented to

the Faculty of the Department of Chemical and Biomolecular Engineering

University of Houston

In Partial Fulfillment

of the Requirements for the Degree

Master of Science

in Chemical Engineering

by

Ogochukwu Yvonne Enekwizu

May 2013

Abstract

The dehydrogenation of ethylbenzene to styrene is explored in a membrane reactor under conditions of hydrogen permeate evacuation. Under typical reaction conditions of high temperature and low pressure, moderate to high conversion and selectivity to styrene are obtained. The employment of a palladium membrane in the reaction system boosts hydrogen product removal thus leading to higher conversions. However, a limited amount of literature exists on experimental results obtained from investigations of ethylbenzene dehydrogenation in composite palladium membrane reactors.

In this study, defect free composite palladium membranes which exhibit good flux behavior at temperatures for ethylbenzene dehydrogenation were synthesized. The membrane reactor was operated in a narrow temperature range characterized by relatively fast kinetics and limited by-product formation. There were, however, several unanticipated difficulties associated with the membrane system which included unfavorable interaction between the palladium surface and reaction species, by-product formation and limited driving force for permeate evacuation. These challenges were further exacerbated when the system was run at elevated pressures. The findings underscore the need for a detailed analysis of the surface chemistry during reaction conditions to gain an understanding of the interactions that persist between the reactant atmosphere and the palladium membrane.

Table of Contents

List of Figures

List of Tables

Chapter 1

Introduction and Objectives

1.1 Palladium Based Membrane Reactors

A membrane reactor can be described as a device in which a chemical reaction and a membrane based purification process occur simultaneously. They are usually applied to thermodynamically limited reactions in a bid to increase conversion and yield beyond their equilibrium values by withdrawing some products while mitigating undesired side reactions that may occur [1]. Mass transport across membranes can be non-permselective or permselective. In the case of the former, all components of a mixed stream permeate at comparable rates depending on their molecular weights. Mass transport across a membrane is permselective when specific components of a mixed stream permeate through the membrane by a solution diffusion mechanism [2].

The unique/singular ability of palladium and its alloys to selectively transport hydrogen has been known and exploited for decades [3 - 5]. This property of the metal has resulted in an increased application of palladium and palladium alloy membranes in the field of gas separation especially for the purification of hydrogen. The clean generation of hydrogen is an important technology for supporting the growing energy demand via fuel cell production. Besides its growing fuel cell applications, palladium membranes are also employed in reactions that require hydrogen removal to overcome thermodynamic limitations and achieve higher conversions. The most notable of such reactions include steam reforming of methane [6 - 7], water-gas shift reaction [8 - 9] and dehydrogenation of hydrocarbons [10 - 12].

The permeation of hydrogen through a metal is dependent on its diffusivity and solubility through it:

$$Q = D \,.\, S \,, \qquad (1 - 1)$$

where D is the diffusivity and S represents the solubility. Since palladium is very permeable to hydrogen and impermeable to other gases, perfect permselectivity can theoretically be attained. This is not so in practice due to the existence of contaminants such as carbon that can penetrate the metal lattice and grain boundaries [2]. Diffusion simply occurs as a result of a chemical potential difference brought about by a partial pressure difference across the metal.

Thus, hydrogen permeation through the palladium membrane occurs via what is termed a solution-diffusion mechanism and is a multi-step process. The steps involved include: gas phase transport to the metal surface, dissociative adsorption onto the surface, absorption of atomic hydrogen into bulk lattice, diffusion from bulk to adjacent face of the metal surface, recombination of hydrogen atoms, associative desorption of hydrogen molecule and transport away from palladium surface. Each one of the seven steps involved may be rate limiting depending on the pressure, temperature, thickness and surface characteristics of the membrane [13]. In general, hydrogen permeation is described by the following equation:

$$J_{H_2} = \frac{Q}{\delta} \left[\left(p_{H_2}^{r} \right)^{n} - \left(p_{H_2}^{p} \right)^{n} \right] = q \, \Delta p_{H_2}^{n} \,, \qquad (1 - 2)$$

where J_{H2} represents the transmembrane hydrogen flux, Q is the permeability, δ is the membrane thickness, p^{r}_{H2} and p^{p}_{H2} are the hydrogen partial pressures in the retentate and permeate respectively, q is the permeance, and n is the hydrogen pressure exponent which

indicates the rate-determining step of hydrogen permeation through the membrane. Its value ranges between 0.5 – 1.Equation (1 - 2) highlights the importance of the membrane thickness: thinner membranes imply higher permeance. The partial pressure difference provides the driving force for hydrogen permeation. When the factor n is equal to 0.5, surface effects are deemed negligible and atomic diffusion through the metal lattice is assumed to be rate limiting [1]. The equation becomes the well-known Sieverts – Fick law. On the premise that the hydrogen pressure exponent, n, is independent of temperature, hydrogen transport through dense palladium films is a temperature activated process. The relationship between hydrogen permeability and temperature follows an Arrhenius behavior and is described by the following expression:

$$Q = Q_O \exp(-E_A/RT), \qquad (1 - 3)$$

where Q_O is the pre-exponential factor, E_A represents the apparent activation energy for membrane transport, R is the universal gas constant and T is the absolute temperature. Thus, where Sieverts-Fick law is valid, equations (1 - 2) and (1 - 3) can be combined and hydrogen transport through a palladium membrane is written as follows:

$$J_{H_2} = q\, e^{-E/RT} \left[\left(p^r_{H_2}\right)^{0.5} - \left(p^p_{H_2}\right)^{0.5} \right], \qquad (1 - 4)$$

Dense palladium membranes have been employed in earlier studies [2] but are limited by the cost of the metal and low hydrogen flux values stemming from high wall thicknesses. The use of porous supports (ceramic, metal or glass) for supporting thin palladium films has the obvious advantage of increased flux. Hollow fiber membranes of diameter ca. 2mm and smaller diameter tubes (< 4 mm), in particular, offer high packing densities, withstand high pressure operation and allow flexibility in system design and operation [5,13]. The Harold group has worked extensively with these membranes with good results [5, 14, 15]. As

mentioned earlier, membrane reactor studies have been conducted on several reactions. Very important and widely investigated classes are those involving the dehydrogenation of hydrocarbons. The reactions of great industrial interest [16] are dehydrogenation of: $C_2 – C_5$ alkanes to their corresponding alkenes [17], $C_{10} – C_{15}$ linear alkanes needed for the synthesis of linear alkylbenzene (LAB) [18] and ethylbenzene to styrene [19].

1.2 Ethylbenzene Dehydrogenation to Styrene

Styrene, a commodity chemical used to make thousands of industrial, commercial, household and personal articles, is one of the most important and versatile monomers in the petrochemical industry. As of 2010, the global production of styrene was about 25 million metric tons [20]. Ethylbenzene dehydrogenation is the more common of the two methods used for commercial styrene manufacture, accounting for over 90% of styrene production. The other process involves the co-production with propylene oxide [21]. The dehydrogenation reaction is endothermic and takes place over a promoted iron-oxide catalyst in a fixed bed reactor at temperatures ranging between 550-650°C in the presence of copious amounts of steam and is described by the following equations:

$$C_6H_5CH_2CH_3 \leftrightarrow C_6H_5CHCH_2 + H_2 \qquad \Delta H_o = 117 \text{ kJ/ mol}, \quad (1 - 5)$$

$$r_1 = k_1\left(P_{EB} - \frac{P_{ST}P_{H2}}{K_P}\right), \qquad (1 - 6)$$

$$K_P = exp\left(\frac{-\Delta G^o}{RT}\right), \qquad (1 - 7)$$

where r and k are the reaction rate and reaction rate constant, P_{EB}, P_{ST} and P_{H2} are the partial pressures of ethylbenzene, styrene and hydrogen, respectively, K_P is the equilibrium constant, and ΔG^o is the standard state free energy change.

From the stoichiometry presented above, it is evident that the reaction is limited by thermodynamic equilibrium. Operation at lower pressures favors the production of styrene. Being endothermic, high temperature increases the equilibrium conversion but also gives rise to an increase in unwanted side reactions. These side reactions yield by products that decrease the styrene selectivity, the most significant contributions being from the formation of toluene and benzene:

$$C_6H_5CH_2CH_3 + H_2 \rightarrow C_6H_5CH_3 + CH_4\,, \qquad (1 - 8)$$

$$C_6H_5CHCH_2 + 2H_2 \rightarrow C_6H_5CH_3 + CH_4\,, \qquad (1 - 9)$$

$$C_6H_5CH_2CH_3 \rightarrow C_6H_6 + C_2H_4\,. \qquad (1 - 10)$$

Other by-products include carbon dioxide, methane, ethylene, phenylacetylene, α-methylstyrene, cumene and other heavy aromatics [21].

Commercial dehydrogenation catalysts are primarily comprised of iron oxide promoted by potassium. Other metals are used as supplementary promoters and include oxides of chromium, cerium, molybdenum, calcium and magnesium. Potassium plays a very important role in the catalyst as it increases the reaction rate by an order of magnitude. It is also volatile and under reaction conditions redistributes itself within catalyst particles [16, 22].

A considerable amount of coking/carbonaceous deposition occurs during reaction which reduces catalytic activity and decelerates ethylbenzene conversion. Carbon is formed from the cracking of alkyl groups on the aromatic ring of the ethylbenzene molecule [21]. The presence of steam in large molar excess helps to retard this effect via gasification and the water gas shift reactions:

$$C + H_2O \rightarrow CO + H_2 , \quad (1 - 11)$$

$$CO + H_2O \leftrightarrow CO_2 + H_2 , \quad (1 - 12)$$

Steam also provides part of the heat required to maintain reaction temperature and acts as a diluent, thus effectively shifting the equilibrium towards more styrene production. This is evident from equation (1 – 6) when the partial pressures are defined in terms of molar flow rates to give the following expression:

$$K_P = \frac{P}{F_T}\left(\frac{F_{EBo}X_{EB}^2}{1- X_{EB}}\right), \quad (1 – 13)$$

where the total molar flow rate F_T is defined as:

$$F_T = F_{EBo} + F_{steamo} + F_{EBo}X_{EB} . \quad (1 – 14)$$

Solving equation (1 – 13) for the ethylbenzene conversion, X_{EB}, emphasizes the role of steam in the dehydrogenation reaction. This is better illustrated in Figure 1 – 1 where ethylbenzene conversion is plotted as a function of temperature for various steam to hydrocarbon ratios. The minimum steam to hydrocarbon ratio required for most catalysts ranges from 7 – 10. Intensive research efforts have been made to get this ratio to a much lower value by adjusting catalyst compositions [23 - 24]. Although the presence of steam is beneficial to the dehydrogenation reaction, the amount used is usually constrained by plant economics and cost. To this end, several groups have considered the use of other diluents such as carbon dioxide to address this [24 - 25]. Steam also serves to control the nature of the active state of the iron oxide catalyst under reaction conditions by retarding its reduction to the less active metallic state [27]. This minimizes susceptibility of the catalyst to deterioration and lengthens its lifetime and stability.

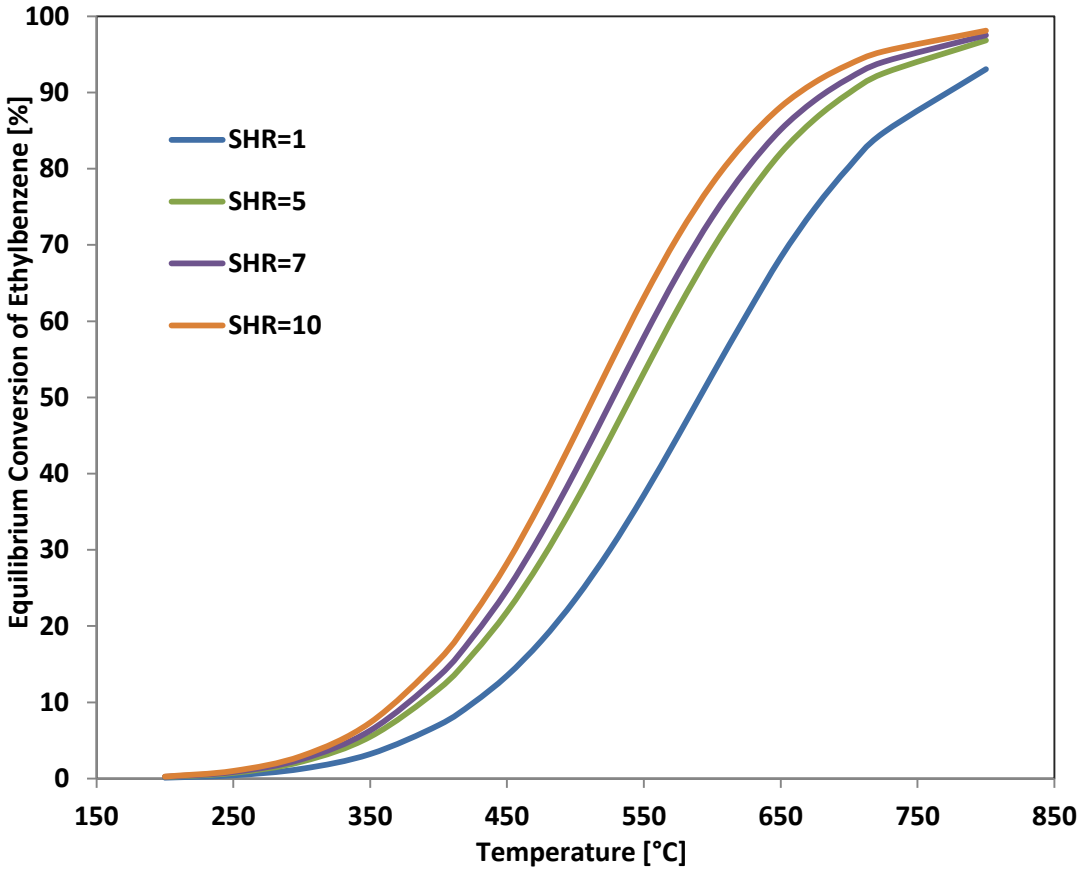

Figure 1 – 1 Dependence of ethylbenzene conversion on steam as a function of temperature.

Styrene plants are typically run under isothermal or adiabatic conditions. In the case of the adiabatic reactor, the heat of reaction is supplied by the superheated steam that is co-fed with ethylbenzene. Multiple reactors in series with interstage heating are used to ensure higher conversions by raising the temperature of the reaction mixture. Reactors that are operated under adiabatic conditions are designed to ensure radial flow thus decreasing pressure drop through the catalyst while providing a large flow area [21]. Most styrene plants opt for this method. Isothermal dehydrogenation is practiced in Europe and Japan by Lurgi and BASF. In principle, isothermal processes have the advantage of saving costs from the excessive use of steam as a source of preheat and maintaining temperature within reasonable

limits at both inlet and outlet sections. However, they are significantly affected by heat transfer limitations. For effective heat transfer from the heating medium, a multitubular design is required and such reactor designs are quite expensive to construct.

1.3 Palladium Membrane Research for Ethylbenzene Dehydrogenation

Being equilibrium limited, energy consuming and of great commercial interest, a strong motivation exists for discerning new methods to increase efficiency and reduce the cost of styrene production [1, 21, 28]. Enhancement of ethylbenzene conversion can be achieved by the selective removal of one of the reaction products (hydrogen) while the reaction is occurring. The reaction may then be limited by the kinetics associated with the reaction system or with the catalyst.

Several studies have been conducted on membrane reactors for this purpose; however, there is limited experimental data with regards to the use of palladium membranes for ethylbenzene dehydrogenation. The investigations that have been reported show promising results on the lab scale.

Quicker et al. [12] investigated the dehydrogenation of ethylbenzene in a palladium alumina membrane reactor. For a temperature of 580°C and retentate pressure of 1.1 bar, they reported a 15% increase in conversion at the maximum sweep gas flow. Selectivity to styrene stayed constant at about 93% showing that selectivity was not enhanced by the palladium membrane.

She et al. [28] conducted ethylbenzene dehydrogenation studies in a porous stainless steel membrane reactor. Their results indicate a 10% increase in conversion compared to the fixed bed reactor for temperatures greater than 600°C and purge gas to reactant feed ratios greater than 15. They also reported an increase in styrene selectivity from 1% to about 15%

in the membrane reactor for the range of contact times considered. Pressure was maintained at 1.2 atm for all experiments conducted.

Elnashaie et al. [29] employed a multitubular palladium membrane module where each membrane had a thickness of 0.5 μm. Two different membrane configurations were used: fixed bed and fluidized bed. Their results indicate that the membrane reactors performed a lot better than their fixed bed and fluidized bed counterparts achieving an increase of about 12 – 36% in ethylbenzene conversion for the various catalysts they studied. They also reported to have achieved enhancement in styrene yield as high as 26.5%.

Yu and Xu [19] were able to achieve conversions above equilibrium by employing a 10μm palladium membrane. At a pressure of 1.4 atm, temperature of 580°C and 0.36 h^{-1}, they reported a 6.3% increase in conversion compared to thermodynamic equilibrium conversion for the same operating conditions. Their results indicate no improvement on styrene selectivity. It should be mentioned that all the studies were performed with a feed diluted with nitrogen. Despite the successes achieved in these studies, commercial deployment of palladium membranes still face the challenges of insufficient hydrogen flux, permselectivity and continual stability under operating conditions.

1.4 Objectives

Ethylbenzene dehydrogenation to styrene has served as a model for many simulation studies for equilibrium shift in membrane reactors. The main focus in the past has been on commercial type porous membranes that exhibit Knudsen-type separation characteristics [30 - 32]. Only recently experiments involving the use of composite palladium membranes have been reported. Consequently, there is very limited information on the reaction in hydrogen selective membrane reactors. Also, very little or no information is reported concerning

characterization studies on the membranes used before and after the experiments. More importantly, available literature has failed to describe what effects the reactant atmosphere (steam, ethylbenzene) have on the hydrogen flux and membrane stability at higher temperatures.

The effects of these non-hydrogen species on the membrane flux may undermine the transport of hydrogen. Steam is present in large molar quantities; ethylbenzene is a heavy aromatic and a precursor for carbon, a component which is known to have very detrimental effects on the structure and lifetime of the membrane [2]. Therefore, the impact of these gases should be considered before employing a palladium membrane for hydrogen withdrawal. Studies which do account for the effects of water on the palladium membrane are for other reaction systems e.g., methanol steam reforming [33] and focus on small concentrations of water in the feed stream.

This work describes the magnitude of the effects of the reaction species on the hydrogen flux before and after the reaction occurs. Several process parameters (space velocity, pressure, temperature, catalyst size) were also varied to converge on a set of operating conditions for optimal conversion. Most of the previous studies have employed the use of nitrogen/argon as a sweep gas in the feed or on the permeate side of the membrane reactor to provide a driving force for hydrogen permeation. Consequently, multitubular modules or large diameter supports (0.7 – 6 cm) have been used to accommodate this. Favorable results have been reported by Harold et al. [5], Nair et al. [14] and Israni et al. [15] on the use of low diameter supports (0.2 – 0.4 cm) for several reaction systems and these have also been employed here. Thus, studies in this work are focused on the operation of smaller diameter single-tube packed bed membrane reactor under permeate evacuation; i.e.,

without the use of sweep gas. Increased conversion under such conditions is desirable as it eliminates the need for the provision of an inert gas and allows for a pure hydrogen effluent.

The overall goal of this thesis is to carry out a comprehensive analysis on the performance of a palladium membrane reactor under realistic process conditions for ethylbenzene dehydrogenation. The specific objectives are summarized as follows:

(i) Conduct permeation studies to ascertain the effects of reaction species on the transmembrane flux.

(ii) Conduct packed bed reactor studies to gain an understanding of the effects of various operating parameters on the reaction system.

(iii) Investigate the dehydrogenation reaction in a single-tube packed bed membrane reactor under conditions of permeate evacuation.

Chapter 2

Experimental Materials and Methods

2.1 Membrane Synthesis

The hollow fiber ceramic membrane supports used in this study were made of asymmetric α-alumina with a surface pore size of 50nm. The supports had dimensions of 2 mm I.D., 4 mm O.D. and length of 25.4cm (supplied by Media & Process Technology Inc). Electroless plating was used to deposit palladium on the selective membrane layer. Prior to this, the membranes underwent several pretreatment steps.

The ceramic supports were first rinsed with isopropyl alcohol and subsequently with deionized water to remove any contaminants present from the membrane fabrication process. The supports were dried at 120°C in an oven before they were calcined in a box furnace at 650°C for 6hrs with a heating ramp of 1°C/min. This was done to burn off any organic contaminants that may have still adhered to the supports.

To initiate the plating process, a surface activation was done to seed the membrane surface with finely divided palladium crystallites. Surface activation is a key element in the synthesis of the membranes as defects in the palladium film can occur when the membrane is not uniformly activated prior to plating. The activation process involved a two-step immersion sequence in a sensitizing bath ($SnCl_2$) followed by an activating bath ($PdCl_2$). Intermediate deionized water rinses were done between the 5-minute sensitization and activation steps. The membrane surface was activated when it had a dark brown appearance. To prevent activation on the inside surface of the membrane, Teflon tape was wrapped around one end of the membrane while the immersions were done. The compositions for both solutions are given in the Table 1.

Electroless plating involves the deposition of metals such as palladium using chemicals. It is autocatalytic in the sense that the metal being deposited also catalyzes further deposition. The electroless plating bath comprised of a palladium amine complex, the disodium salt of ethylenediamine-tetraacetic acid (disodium salt of EDTA) which served as the stabilizer and hydrazine as the reducing agent. The bath formulation is based on a recipe used by Nair et al. [34] and is shown in Table 1.

The reaction describing this deposition is shown as follows:

$$2Pd(NH_3)_4{}^{2+} + N_2H_4 + 4OH^- \rightarrow 2Pd^0 + 8NH_3 + N_2 + 4H_2O\,, \qquad (2 - 1)$$

The amount of palladium being deposited was monitored by a quartz crystal microbalance (PM-700 Series Maxtek). Plating was halted as soon as the solution turned a milky color which indicated bath decomposition. Decomposition tended to occur more readily at high concentrations of hydrazine and higher temperatures [34]. It is for this reason that plating was conducted multiple times at 35°C till the desired thickness was obtained.

After plating, the membranes were rinsed in deionized water and dried overnight at 120°C in the oven. The thickness of the palladium film was calculated by dividing the weight difference in the plated and unplated membranes by the plated surface area and palladium density.

Table 1-1: Composition of sensitization and activation solutions and electroless plating bath for palladium membrane synthesis

Sensitizing solution		Activating solution	
$SnCl_2$	1.2g/l	$PdCl_2$	0.1g/l
HCl	0.2N	HCl	0.2N
Electroless Plating (ELP) Bath Composition			
$PdCl_2$		5g/l	
NH_4OH (29.5 wt%)		600ml/l	
EDTA.2Na		40g/l	
N_2H_4 (1M)		10ml/l	

2.2 Permeation Measurements

Schematics of the permeation system and the single fiber permeation unit used to investigate the separation capabilities of the palladium membranes are shown in Figures 2-1 and 2-2, respectively. The fiber was fitted co-axially within a 0.57 inch OD stainless steel tube comprising the permeation device with the aid of graphite ferrules and modified Swagelok fittings. One end of the membrane was sealed off and the other left open to ensure evacuation of the permeate stream. Prior to the permeation experiments, a pressure hold test using N_2 was performed to ensure that the membrane and permeation device were leak-free. This room temperature test involved applying a pressure of 70psi on the lumen side of the membrane and monitoring for over 3hours. A constant pressure confirmed that the membrane had satisfactory integrity for the permeation test.

The permeation device was placed within a tube furnace and temperature varied between 400 and 600°C. Temperatures were monitored by inlet by K-type thermocouples positioned at the inlet and outlet points of the separator apparatus. The desired feed gases were ultrahigh purity grade supplied by Matheson TriGas and metered through individual Aalborg mass flow controllers. The liquid streams (ethylbenzene (EB) and water) were introduced to the setup through HPLC syringe pumps and vaporized prior to entry. The inlet

hydrogen flow rate was fixed at 700 sccm so as to maintain a measurable H_2 flow rate through the membrane at all conditions. A Swagelok back pressure regulator was used to control retentate side pressure between 1 and 5 bar absolute. The permeate side was subjected to both atmospheric and vacuum conditions with the aid of a 0.25kW GAST diaphragm pump. A series of valves enabled the analysis of the composition of both retentate and permeate streams by a 6890N Agilent gas chromatograph. Flow rates on both permeate and retentate streams were measured by a digital flow meter (Bios Definer 220).

In the first part of the experiments, pure hydrogen or pure nitrogen were fed to the retentate side of the permeation unit at specific temperatures and pressures in order to ascertain the pure gas permeation properties of the membrane. For these experiments only the flow meter was required to deliver the requisite hydrogen; i.e., no composition measurement was necessary. In the second part of the study, H_2 along with varying concentrations of a second component (N_2, H_2O, EB) were fed to the retentate side to determine the effects of the reaction species on the hydrogen flux. The decrease in flux when compared to pure hydrogen conditions provided this information. Both the flow meter and the GC were used simultaneously to get accurate measurements whilst conducting analysis. The hydrogen stream (700 sccm) was fed continuously to the apparatus and 30 minutes was given upon introduction of each new species before any readings were taken under atmospheric and vacuum conditions, respectively. Once taken, flow of the non-H_2 species was halted and pure H_2 fed till the permeate flow rate achieved a steady state value. For the liquid species, a moisture trap was installed on the exit line of the permeate side to prevent any moisture from getting to the vacuum pump or GC should there be a case of membrane failure. Inlet gas flows, temperatures and pressures were monitored by LABTECH software. Permeation results are reported in terms of H_2 transmembrane flux (mol/m^2s).

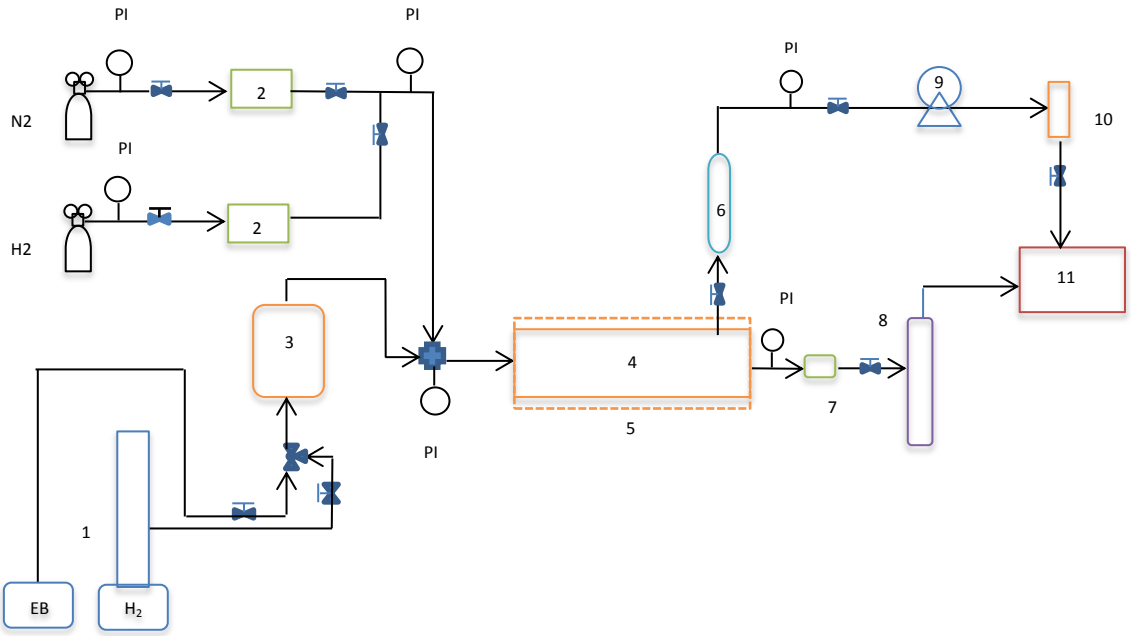

1 – Syringe pump; 2 – Mass Flow Controller; 3 – Preheater; 4 – Reactor; 5 – Furnace; 6 – Moisture Trap; 7 – Back Pressure Regulator; 8 – Cooling Unit; 9 – Vacuum Pump; 10 – Rotameter; 11 – Gas Chromatograph

Figure 2-1 Basic layout of the laboratory permeation and reactor setup.

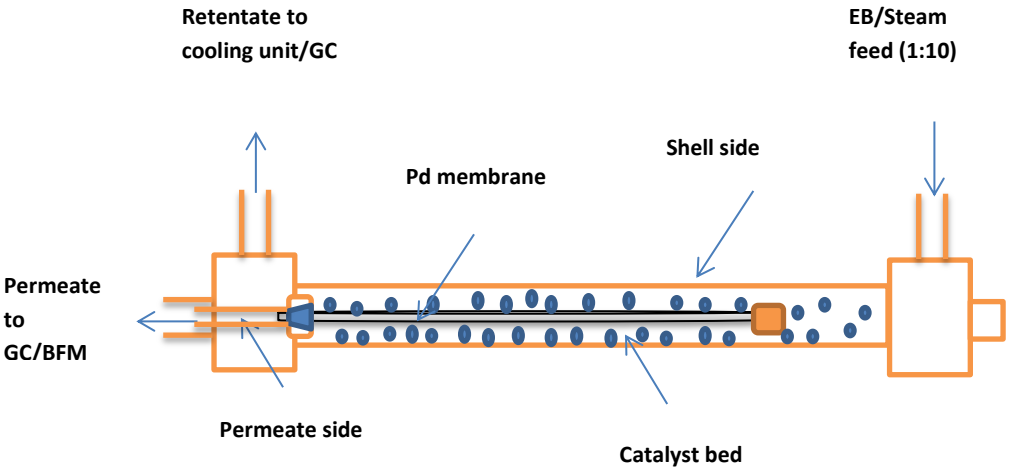

Figure 2-2 Details of the reactor employed for the dehydrogenation studies with the membrane enclosed.

2.3 Reactor Setup

The set up used for the ethylbenzene dehydrogenation reaction in a packed-bed reactor (PBR) and packed-bed membrane reactor (PBMR) is similar to the permeation setup. Ethylbenzene (99.8% Aldirch) and water (de-ionized) were fed through two individual syringe pumps and sent to an evaporator where they were vaporized. The steam and EB mixture was passed through the preheat section which was maintained at 200°C and further heated to reaction temperature upon entry to the catalyst bed. The PBR comprised of a stainless steel tube with 0.575 inch ID and 18 inch length was placed in a furnace. The PBMR was comprised of an identical stainless steel tube, the only difference being that a palladium coated fiber was fitted within co-axially. The palladium membrane was 10 microns thick and 5cm long.

The reactor was packed with catalyst pellets situated between two quartz wool plugs. The catalyst used was a 48 wt% Fe_2O_3 promoted with 10% K_2O and oxides of cerium, magnesium, molybdenum, calcium and sodium provided by TOTAL. The catalyst particles are extrudates of cylindrical shape with a nominal diameter of 3 mm and a bulk density of 1.3 g/cc. 40 g of catalyst was used for the PBR whereas 31g was used for the PBMR. Reaction products exited through the shell side of the setup. The reactor outlet was divided into two streams. The larger stream was sent to a heat exchanger where ice water was used as a cooling medium to condense the liquid products. The liquid product was sampled once collected. The other stream was sent directly to the gas chromatograph via a heat traced line.

The gas chromatograph employed for analysis is a 6890N Agilent GC equipped with a time programmable valve system that facilitates the injection of the product gases and swaps valves in a timely manner between columns. This enables peaks of interest from one column

to be cut onto another column that possesses a different stationary phase for separation of the chemical species being considered. The columns employed in the GC are:

- Stabilwax: Fused Silica capillary column (separation of aromatic compounds)
- MolSieve 5A: Micropacked GC column (separation of N_2, H_2, O_2, CH_4, CO)
- HayeSep T: Packed GC column (separation of CO_2 and H_2O and guard for Molsieve column)

A schematic for the configuration of switching valves and columns employed is shown in Figure 2-3 below with helium used as a carrier gas:

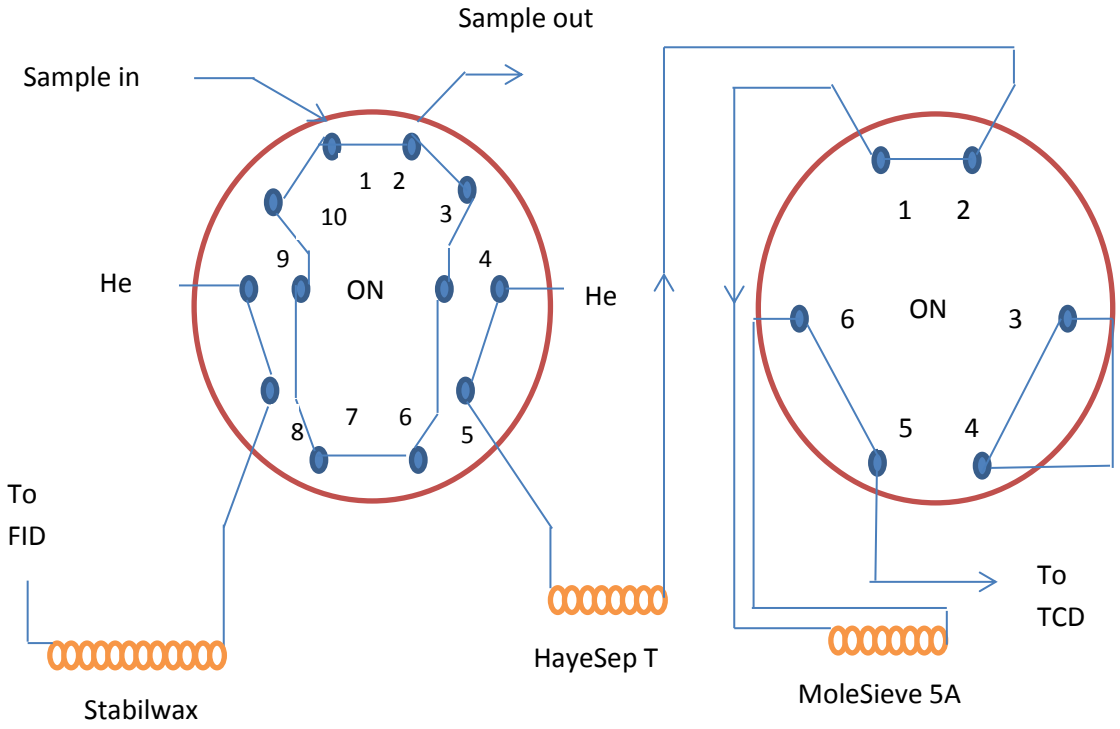

Figure 2-3 Schematic of valve switching system and columns.

Eluting compounds were identified by two detectors: a flame ionization detector (FID) for analysis and quantification of the organics (benzene, toluene, ethylbenzene, cumene

and styrene) and a thermal conductivity detector (TCD) for analysis of the gas phase products (hydrogen, methane, carbon monoxide). For calibration purposes, 5 liquid standard mixtures with known concentrations spanning the expected composition of the effluent stream were fed to the GC with high precision Hamilton syringes and analyzed.

The reactions were performed at temperatures ranging from 450 to 600°C, total catalyst side pressures ranging from atmospheric to 5bar and a steam hydrocarbon ration (SHR) of 10:1. The reactor was operated under essentially isothermal conditions confirmed by thermocouple measurements placed at the inlet and outlet sections of the reactor. In the PBMR experiments the permeate side was open to atmosphere through the GC or digital flow meter or subjected to vacuum. The EB feed was varied between 0.1ml/min to 0.4ml/min to span a range of space velocities.

Each run required 3hrs after the feed was introduced to achieve a steady state as determined by the stabilization of exit concentrations and temperatures. Once a particular run ended, the next run was initiated by changing the required parameter. No prior activation procedure was required for the catalyst. The catalyst bed was always kept under a stream of nitrogen overnight and when experiments were not being conducted. At the end of the PBMR experiments, pure hydrogen gas and mixtures of nitrogen and hydrogen gas were fed to the reactor to ascertain the membrane's stability and separation capabilities after being subjected to the reactant atmosphere.

Chapter 3

Results and Discussion

3.1 Permeation Studies

3.1.1 Pure gas permeation studies

The permeation features of the top layer membrane were measured in the permeation apparatus described in Chapter 3. The simple pressure hold experiments conducted showed that the tubular membranes were of good quality and have a uniform coating of palladium firmly adhered to the alpha alumina substrate. When the retentate side was pressurized with pure nitrogen, no transmembrane nitrogen flux was observed showing that the palladium membrane had a very high selectivity for hydrogen (i.e., at least within our ability to detect pressure change over the particular time period of 4hours). Figure 3-1 illustrates the pure gas permeation characteristics of an 11μm thick composite palladium membrane in terms of hydrogen flux as a function of the difference of the square root of the retentate and permeate hydrogen partial pressure. The permeate side was kept at ambient pressure conditions. The hydrogen flux is in the range of 0.2 – 0.8 mol/m^2s for temperatures ranging from 400 to 600°C. A maximum hydrogen flux of 0.88 mol/m^2s was obtained at 600°C for an overall transmembrane pressure difference of 4bar. The linear dependence in the flux with respect to the square root pressure difference for the entire temperature range shows that the permeation follows Sievert's law for which the diffusion of atomic hydrogen through palladium is rate limiting [2].

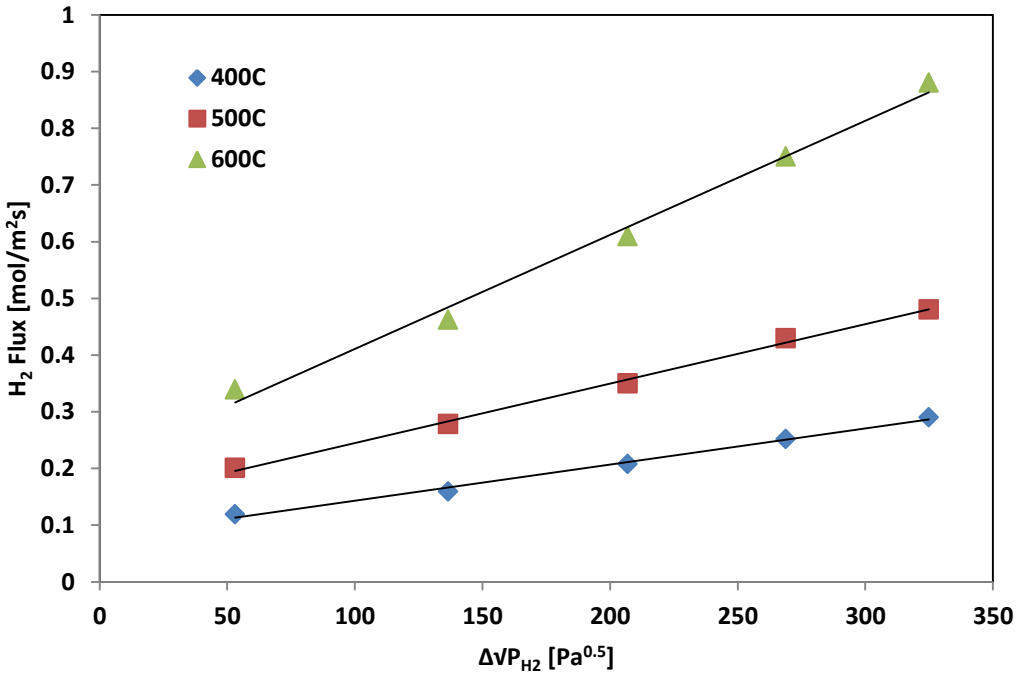

Figure 3-1 Pure hydrogen permeation results for an 11μm palladium membrane.

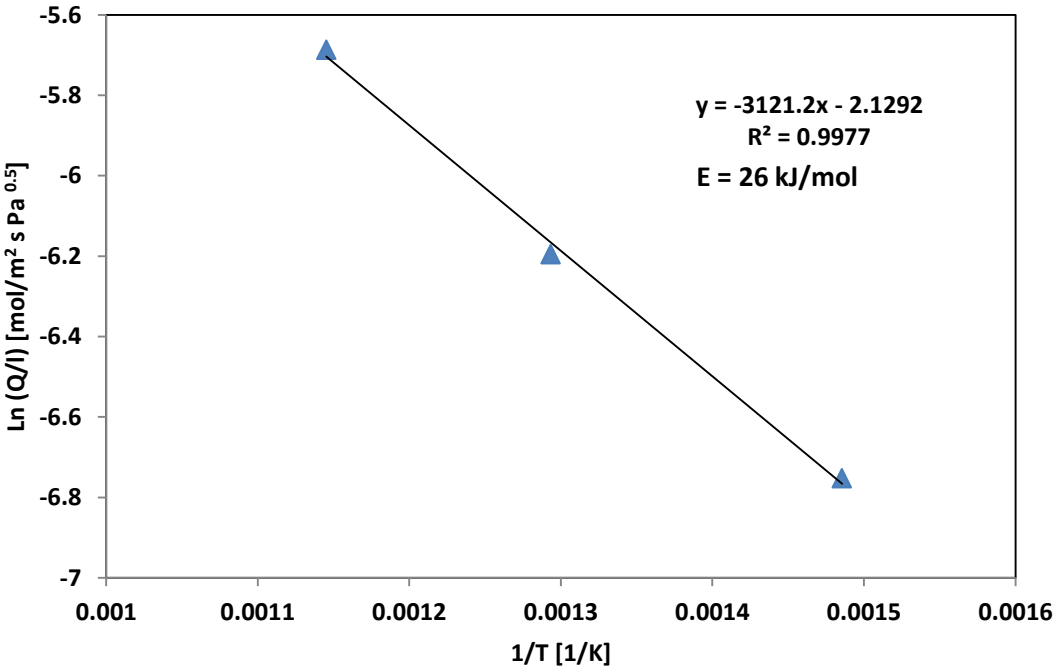

Figure 3-2 Arrhenius plot of the hydrogen permeance of an 11μm thick palladium-alumina composite membrane.

As stated earlier, the transport of hydrogen through a dense palladium film is an activated process. Flux data obtained for temperatures ranging from 400 – 600°C were used to estimate the permeance pre-exponential factor and activation energy. The dependence of the permeance on the temperature follows an Arrhenius relationship as seen in Figure 3-2. The activation energy determined for this study was about 26kJ/mol with permeability ranging between 1.24 – 3.60 mol/m s $Pa^{0.5}$. Other studies have reported activation energies ranging from 10 – 30kJ/mol [1, 15, 34] for similar palladium membranes. The permeation performance compares favorably with membranes from previous studies (see Table 3-1).

Table 3-1 Comparison of permeation results with selected literature data

Membrane	**Comments**	**Thickness [µm]**	**Driving force ΔP_{H2}[kPa]**	**T [K]**	**H_2 Flux [mol/m^2 s]**	**Permeance [mol/m^2 s Pa]**	**Ref.**
Pd/Al_2O_3	ELP	7-15	100	673	0.31-0.48	3.10×10^{-6}	[1]
$Pd/\alpha\text{-}Al_2O_3$	ELP Binary gas permeation	13	100	687	0.06	6.0×10^{-7}	[34]
$Pd/\gamma\text{-}Al_2O_3$	ELP Pure gas permeation	5	400	780	0.52	1.3×10^{-6}	[34]
Pd/Al_2O_3	ELP	3	-	673-873	0.04	4×10^{-7}	[12]
Pd/Al_2O_3	ELP	10	-	773	0.4	3.9×10^{-6}	[19]
$Pd/\alpha\text{-}Al_2O_3$	ELP Pure gas permeation	11	400	773-873	0.5-0.9	1.41×10^{-6}	This work
$Pd/\alpha\text{-}Al_2O_3$	ELP Binary gas permeation	11	100	873	0.199	1.79×10^{-6}	This work

The permeation flux increases with transmembrane pressure difference of the H_2 permeate. This can be achieved either by increasing the retentate pressure or decreasing the permeate side pressure. In Figure 3-3, the results obtained at 400°C for pure hydrogen flux are compared for permeate side maintained under atmospheric and vacuum conditions respectively. Determination of the flux for the vacuum-assisted experiments was performed at permeate side total pressures of 34.6kPa. Permeate evacuation made it possible to achieve much higher fluxes for the same applied retentate pressure as seen in the figure below though studies conducted by [1] reported no significant change in the flux when the permeate side pressure was decreased. This flux increase is highly desirable especially for dehydrogenation reactions where high pressure operation is unfavorable. However, for a similar transmembrane pressure difference, flux obtained at atmospheric pressure was slightly higher.

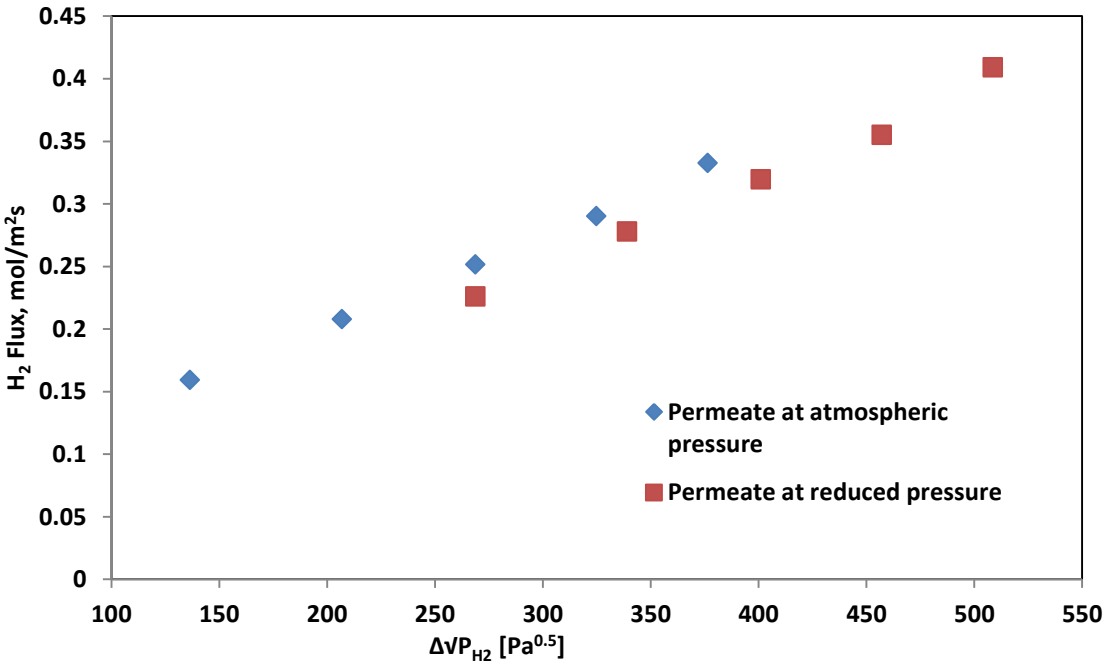

Figure 3-3 Comparison of transmembrane hydrogen fluxes obtained at reduced permeate pressure with measurements at atmospheric pressure for an 11 μm palladium membrane at 400°C.

3.1.2 Binary gas permeation studies

Figure 3-4 compares the binary gas permeation characteristics of the membrane when the feed consisted of 50/50 mixture of hydrogen/nitrogen ,and hydrogen/water, respectively, at 600°C for retentate partial pressures ranging between 1.0 – 2.5 bar (ΔP_{H2} ~ 5 – 140 kPa). For these measurements the permeate side was maintained at ambient total pressure.

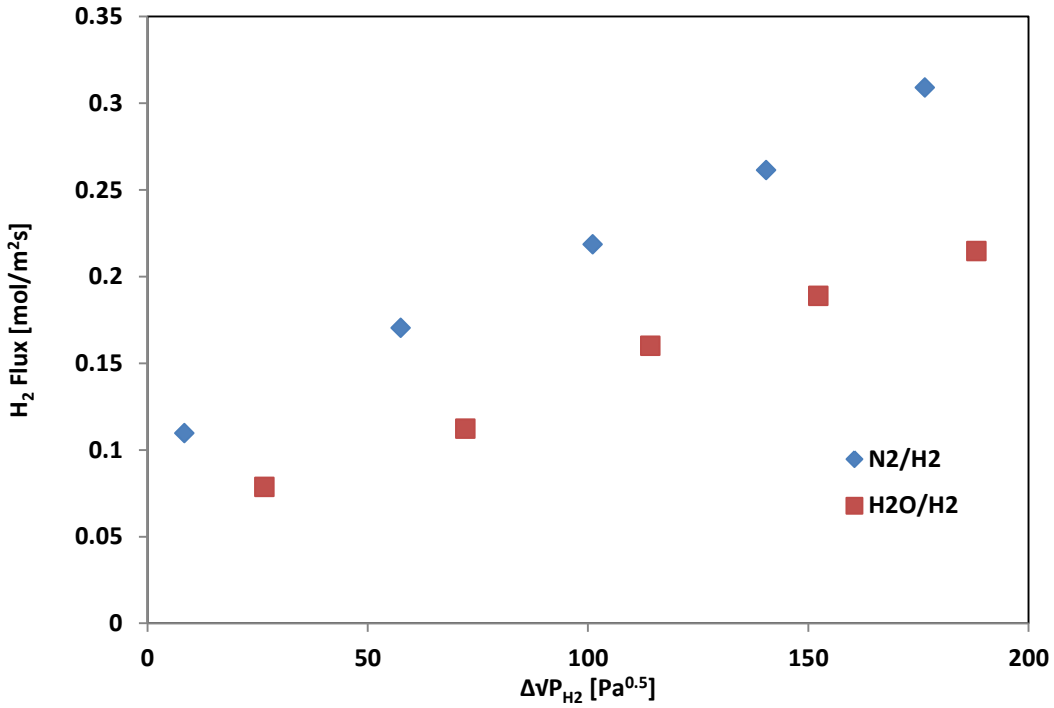

Figure 3-4 Comparison of binary flux results for an equimolar feed of N_2 & H_2 with an equimolar feed of H_2 & H_2O at 600°C for an 11 μm composite palladium membrane.

Hydrogen flux obtained was in the range 0.11 – 0.31 mol/m^2 s for an equimolar mixture of H_2 and N_2. The flux data obtained is comparable to the values reported by other groups at comparable temperature and driving force [1, 35, 36]. Although water is of a lower molecular weight than nitrogen, a lower hydrogen flux (0.08 – 0.22 mol/m^2 s) was obtained for the water/hydrogen mixture. This indicates that water may have an additional effect on the pure hydrogen flux besides a reduction in the hydrogen partial pressure. Such an effect

was reported by Israni and Harold [33]. The flux decrease caused by water on hydrogen will be further explained in the next section.

Studies were also carried out on the equimolar hydrogen/nitrogen and hydrogen/water mixtures with permeate evacuation (see Figure 3-5). The permeate side was maintained at a pressure of 34.6kPa for all runs. A slight increase was observed in the hydrogen flux for both mixtures. The hydrogen flux for the mixture with nitrogen increased vs. the ambient total pressure experiment to 0.21 – 0.38 mol/m^2 s for Δp_{H2} ~ 73 – 208 kPa, whereas that for the mixture with water increased to 0.17 – 0.31 mol/m^2 s for the same transmembrane difference. These results further serve to show that permeate evacuation has a favorable effect on the hydrogen flux which can be exploited in dehydrogenation reactions as earlier stated.

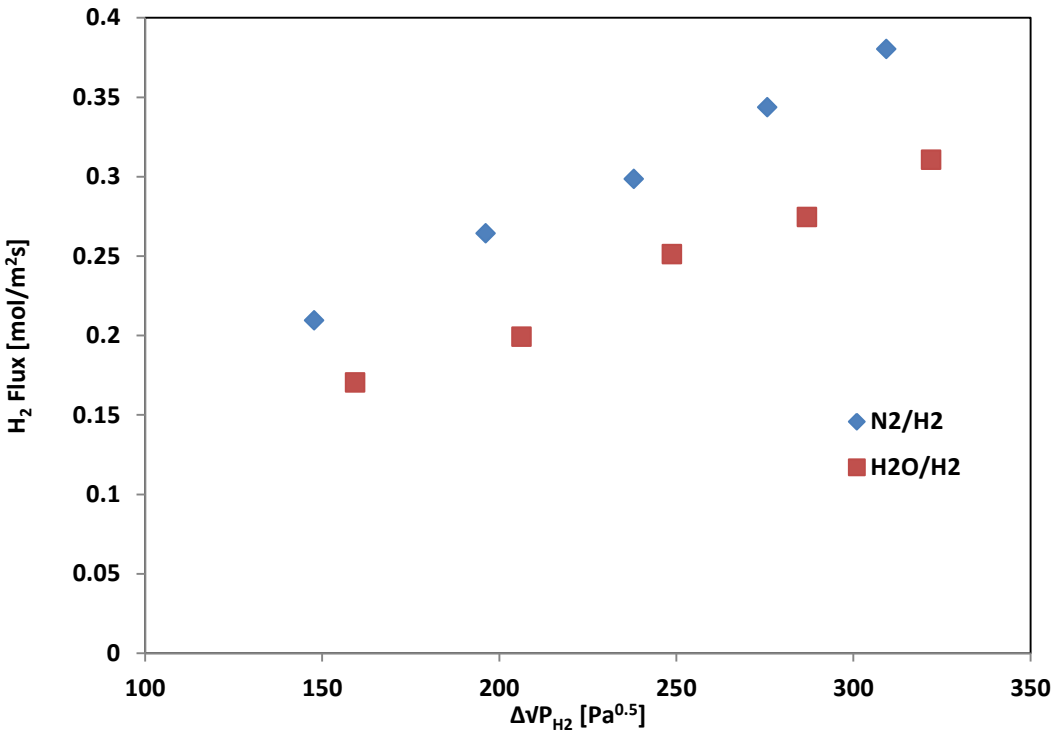

Figure 3-5 Comparison of binary flux results for an equimolar feed of N_2 & H_2 with an equimolar feed of H_2 & H_2O at reduced permeate pressure for an 11 μm composite palladium membrane. Temperature is at 600°C.

3.1.3 Effect of reaction species

Figures 3-6 and 3-7 illustrate the effect of feed impurity on the transmembrane hydrogen flux. In Figure 3-6, the H_2 flux reduction due to the presence of each non-hydrogen species is shown as a function of the mole percent impurity of the feed species at 600°C and 5 bar retentate pressure. Figure 3-7 shows the pure gas permeation results obtained after feeding the membrane with each impurity mixture being considered. The concentrations of each species chosen span values that could be encountered in practice.

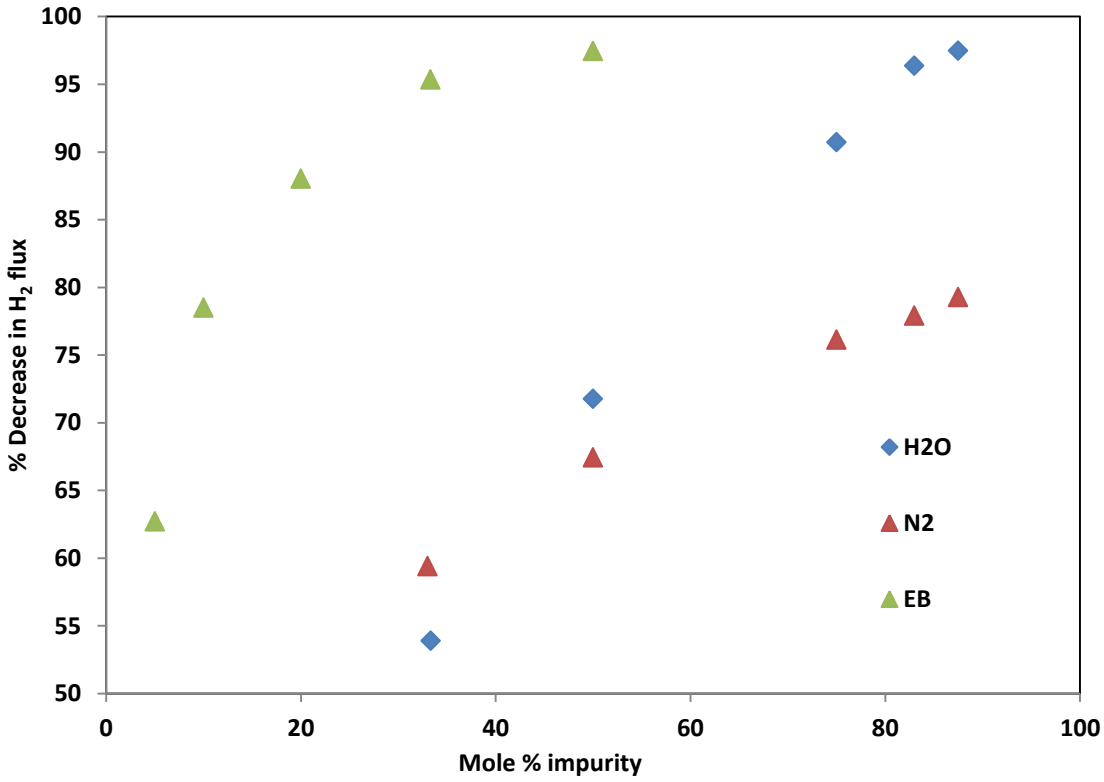

Figure 3-6 Decrease in hydrogen flux due to the presence of N_2, H_2O and $C_6H_5CH_2CH_3$ at 600°C and 5 bar retentate pressure.

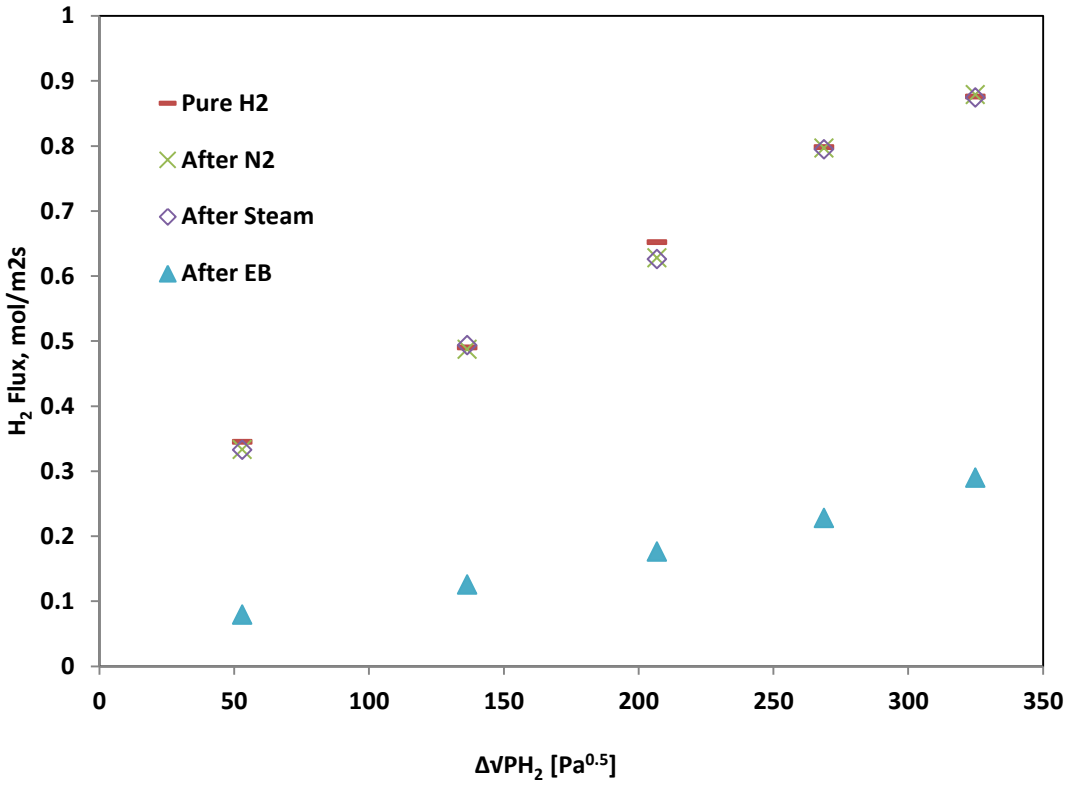

Figure 3-7 Comparison of the influence of N_2, H_2O and $C_6H_5CH_2CH_3$ on transmembrane hydrogen flux at 600°C.

Although N_2 is not an expected feed species for the ethylbenzene to styrene application, it was used to show the effect of a non-adsorbing component on the hydrogen flux; i.e., an inert species. Any decrease in hydrogen flux due to the presence of species other than N_2 is assumed to be as a result of competitive adsorption of the other species with hydrogen on the membrane surface. The main reason for the decrease in flux due to N_2 is attributed to be a result of hydrogen dilution on the feed side and concentration polarization [37]. Concentration polarization results in the buildup of a hydrogen deficient layer adjacent to the membrane due to mass transport limitations [37 - 38].

An increase in the selective permeation of hydrogen leads to an increase in partial pressure of N_2 near the membrane. The combined dilution and concentration polarization

effects lower the hydrogen partial pressure difference which leads to a reduced hydrogen flux. The observed flux reduction is a linear function of increasing N_2 concentration. This is in good agreement with the work done by Nair and Harold [38] who reported that increasing hydrogen feed concentrations reduced the effect of concentration polarization for the same transmembrane pressure difference. Since N_2 is non-adsorbing, the maximum hydrogen permeability was restored once the flow of nitrogen ceased as seen in Figure 3-7.

The presence of water in the system caused an appreciable decrease in flux. It has already been established that less volatile species such as water reduce the amount of adsorbed hydrogen by vying competitively for hydrogen dissociation sites on the palladium surface [33, 39, 40] although there have been conflicting views on the extent of this effect. While some groups report the effect of feed dilution with steam to be significant, due in part to a higher adsorption capacity than other poisons such as CO and CO_2 [37, 41, 42], others indicate the contrary [43 – 44]. Most authors have not measured any inhibitive effect of steam on hydrogen permeance at temperatures greater than 450°C nor at very high steam concentrations partly because those experiments were based on the conditions for steam reforming of light hydrocarbons and water gas shift reactions [37, 39, 41, 42].

In this study, flux reduction due to the presence of steam showed an unusual trend with its concentration in the feed stream (see Figure 3-6). At low concentrations, the effect of water on the flux was less than that of N_2. This may be attributed to nitrogen having a higher molecular weight than water and hence would be a result of the aforementioned concentration polarization effect. A 33% mol feed concentration of water caused a drop of about 54%. However, as the concentrations increased, the effect of water on the flux exceeded that of N_2 with the flux dependence becoming a nonlinear function of the water partial pressure. This may show a transition from diffusion-limited permeation (higher

permeation levels) to surface-limited permeation (lower permeation levels). Moreover, it may suggest that at very high concentrations water adspecies occupies more than one site on the palladium surface, as previously shown in the work of Israni and Harold [33]. A maximum flux reduction of 97.4% was observed at a feed composition of 87% mol water and 13% mol hydrogen which corresponds to the water concentration range of interest for ethylbenzene dehydrogenation. Hydrogen permeability was once again restored to its initial value on halting the steam feed, showing that its effect on permeability was as a result of a reversible competitive adsorption and not poisoning.

The presence of ethylbenzene caused the largest drop in hydrogen flux at all concentrations considered. The flux decrease due to ethylbenzene was strongly nonlinear with respect to the ethylbenzene partial pressure, indicating that the aromatic hydrocarbon makes unavailable multiple surface sites for hydrogen adsorption. It was previously reported by Yoshida et al. [45] and Itoh et al. [46] that mixtures containing saturated/unsaturated paraffinic hydrocarbons exhibited no significant poisoning effects on the flux of H_2 through palladium or its alloys. On the other hand, Paglieri and Way [2], Stachurski and Frackiewicz [47], Ali et al. [48] Jung et al. [49] and Sato et al. [50] all reported that the chemisorption of unsaturated olefins/higher hydrocarbons such as aromatics can cause complete deactivation of surface sites for hydrogen permeation through the membrane and may permanently change the membrane structure. From Figure 3-6, we see that as little as 5 mol% of hydrocarbon impurity in the feed was enough to decrease the flux by 63%. A significant amount of coking was also observed in the outlet stream indicating ethylbenzene decomposition and the formation of a contaminating carbonaceous layer. This presents a serious problem especially when the hydrocarbon content is of an appreciable amount and is the reason why ethylbenzene is usually fed along with copious quantities of steam to reduce the coking

which occurs simultaneously with the reaction [21]. Carbon has been known to degrade palladium membranes by dissolving into the metal lattice via an activated diffusion mechanism causing the membrane to delaminate from its support [2, 50]. A maximum flux drop of 97.4% was observed for a feed composition of 50% mol water and ethylbenzene respectively.

The hydrogen permeation readings taken after illustrate the strong poisoning and surface deactivation effects of the hydrocarbon (see Figure 3-7). The hydrogen flux dropped from 0.88 to 0.29 mol/m^{2}s for the same total transmembrane difference of 4 bar. Attempts to restore the hydrogen permeability by dosing steam in small amounts showed a little improvement though the original flux values were not restored (see Figure 3-8).

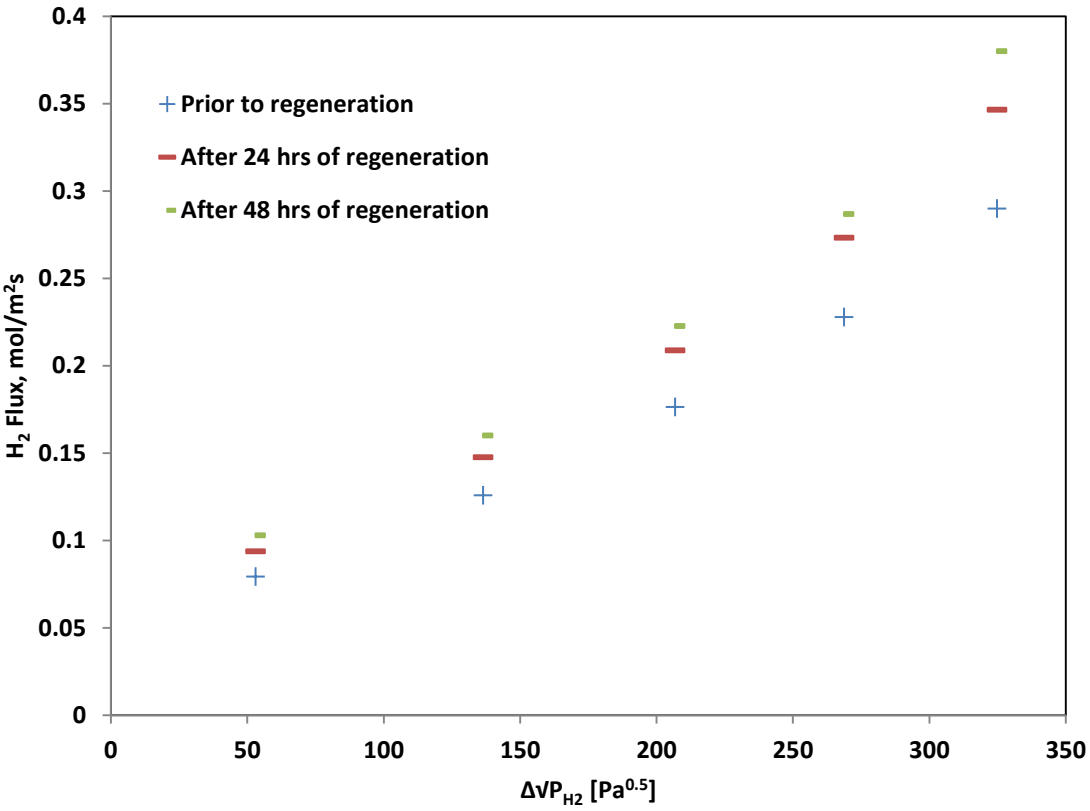

Figure 3-8 Results of pure gas permeations with hydrogen after regeneration under steam at 600°C.

It is believed that flux values close initial results could have been attained if the regeneration procedure was protracted. On removal of the membrane from the permeation device, a significant amount of sooty deposit was observed on the film surface. There were also a large number of pinholes of the surface and what appeared to be swelling/distortion on one end of the fiber.

3.2 Packed bed reactor studies

3.2.1 Equilibrium Conversion

As shown earlier, the following reactions occur during ethylbenzene dehydrogenation:

$$EB \leftrightarrow ST + H_2 \qquad \Delta H = 117.44\frac{kj}{mol} \qquad K_1 = \left(\frac{[P_{ST}][P_{H2}]}{[P_{EB}]}\right), \qquad (3-1)$$

$$EB \leftrightarrow B + C_2H_4 \qquad \Delta H = 105.52\frac{kj}{mol} \qquad K_2 = \left(\frac{[P_B][P_E]}{[P_{EB}]}\right), \qquad (3-2)$$

$$EB + H_2 \leftrightarrow T + CH_4 \qquad \Delta H = -54.27\frac{kj}{mol} \qquad K_3 = \left(\frac{[P_T][P_M]}{[P_{EB}][P_{H2}]}\right). \qquad (3-3)$$

The equilibrium conversion of ethylbenzene to styrene obtained from equation (3 – 1) was plotted as a function of temperature for a steam to hydrocarbon ratio of 10:1 to illustrate the effects of the existing side reactions (equations (3 – 2) and (3 – 3)) on ethylbenzene conversion. From Figure (3-9), it can be observed that the inclusion of the side reactions caused conversion to styrene (X_styrene) to deviate from the typical behavior exhibited by endothermic reversible reactions (X_ideal). This is because it is largely influenced by the side reaction which results in the formation of toluene ($K_3 >> K_2 > K_1$). Hydrogen produced from ethylbenzene dehydrogenation in equation (3 – 1) is used up immediately in the toluene side

reaction causing equilibrium conversion to styrene and toluene to equal each other over a wide range of temperatures.

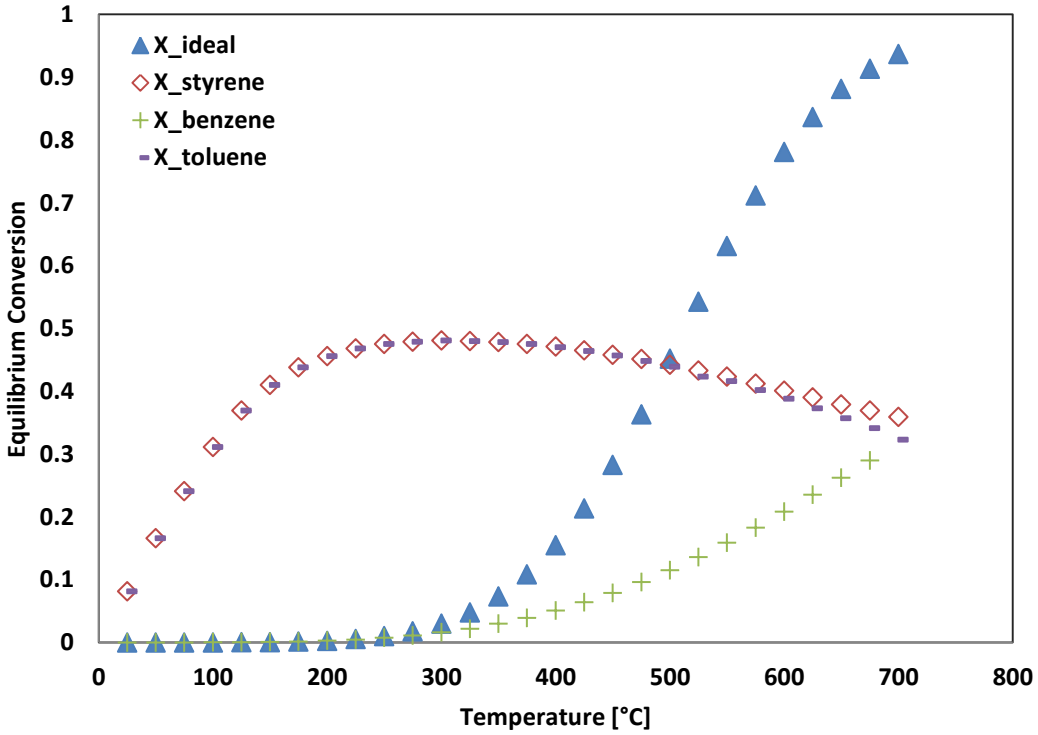

Figure 3-9 Effect of side reactions on equilibrium conversion of ethylbenzene as a function of temperature.

The elimination of the benzene side reaction does little to change this trend showing its effect is not as strong as that of toluene (see Figure 3-10). However, in the high temperature region (> 550°C), we observe that conversion to styrene starts to increase (endothermic behavior) whereas toluene formation begins to drop (exothermic trend).

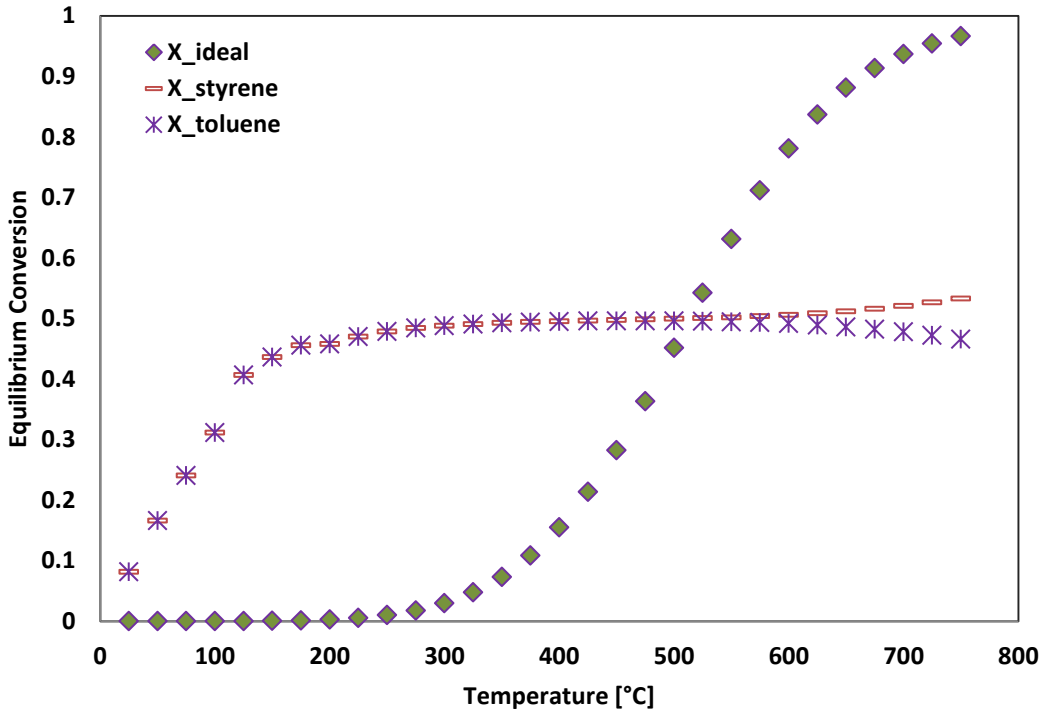

Figure 3 – 10 Effect of toluene side reaction on equilibrium conversion of ethylbenzene.

A sensitivity analysis was also performed to further examine the influence of the toluene side reaction on the ethylbenzene conversion to styrene by adjusting the value of the equilibrium constant for the reaction, K_3. The new K_3 values were obtained using the van't Hoff equation:

$$K_3(T) = K_3(T_r)\exp\left[\frac{\Delta H}{R}\left(\frac{1}{T_r} - \frac{1}{T}\right)\right], \qquad (3-4)$$

where 873K was chosen as the reference temperature (T_r). In the first case, a very low value (K_3 (T_r) = 0.001) was chosen to mimic a situation where toluene formation is minimal or virtually non-existent. With reactant formation favored, this behavior is akin to the ideal situation where no side reactions occur (see Figure 3 – 11). However, as the equilibrium constant is increased (K_3 (T_r) = 10), the influence of toluene formation comes into play and we begin to observe a departure from X_ideal to X_actual.

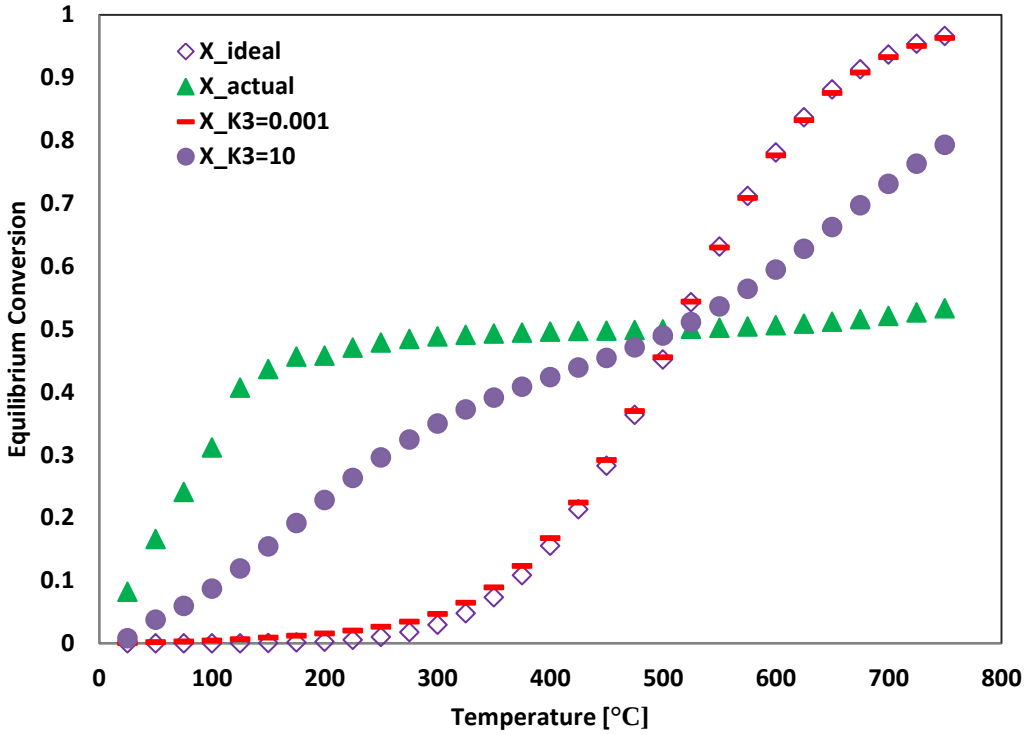

Figure 3 – 11 Sensitivity of ethylbenzene equilibrium conversion to toluene formation.

3.2.2 Effect of contact time

Two catalyst sizes were examined in this study: conventional extruded pellets of 3mm diameter with a bulk density of 1.3g/cc and fine catalyst particles of 8 – 16 mesh (1.18 - 2.36mm) with a bulk density of 1.5 g/cc obtained by crushing the original pellets. The effect of contact time on conversion was determined by carrying out the dehydrogenation reaction in the fixed bed reactor for the two catalyst sizes. Variation in contact time was achieved by changing reactant feed flow rates. Data was collected by injecting samples 3 times into the GC setup. The values plotted in the following figures were averaged.

Figures 3-12 and 3-13 illustrate the steady state conversion as a function of contact time at 625°C for the conventional pellets and at 600°C for the catalyst particles. The

calculated equilibrium conversions are 84% and 78%, respectively, with the total absolute gauge pressure inside the reactor kept at 0 psig for all the experiments.

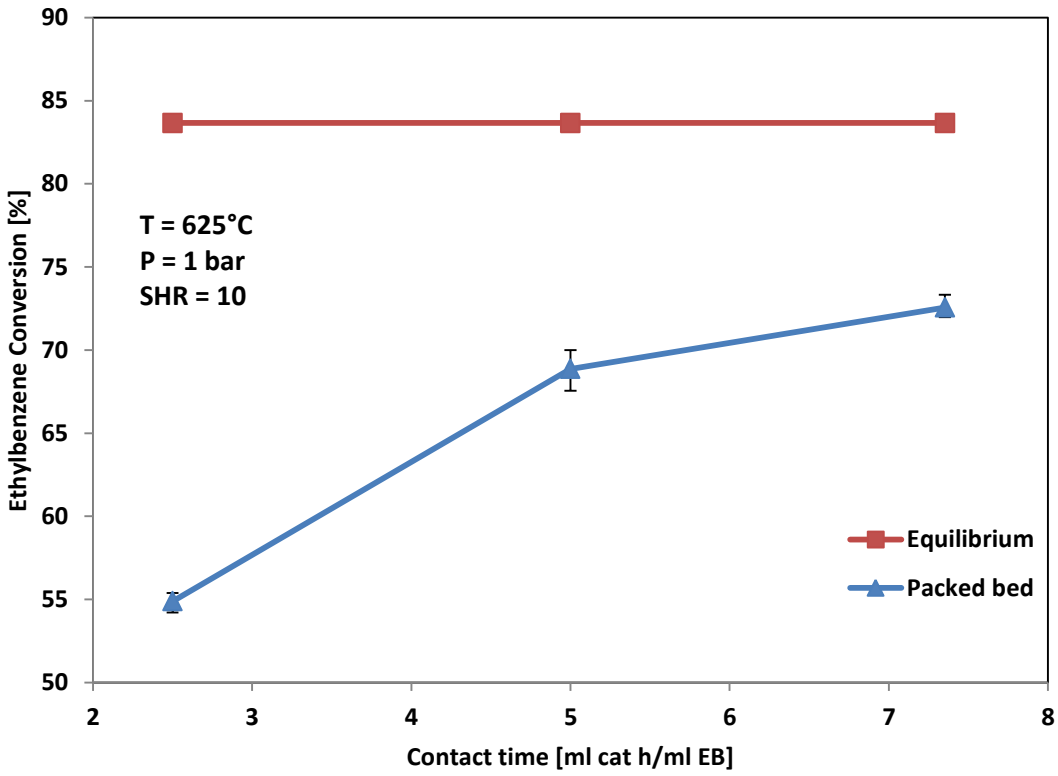

Figure 3-12 Variation of exit conversion of ethylbenzene as a function of contact time for 625°C and 1 bar pressure pellet sized catalyst.

In the case of the fine catalyst particles, conversion was essentially constant for contact times exceeding 2.25 ml cat hr/ml EB as seen in Figure 3-13. For the full size pellets, the trend exhibited in Figure 3-9 suggests that conversion may not have attained a constant value though it was not possible to confirm this by conducting experiments at higher contact times due to equipment limitations.

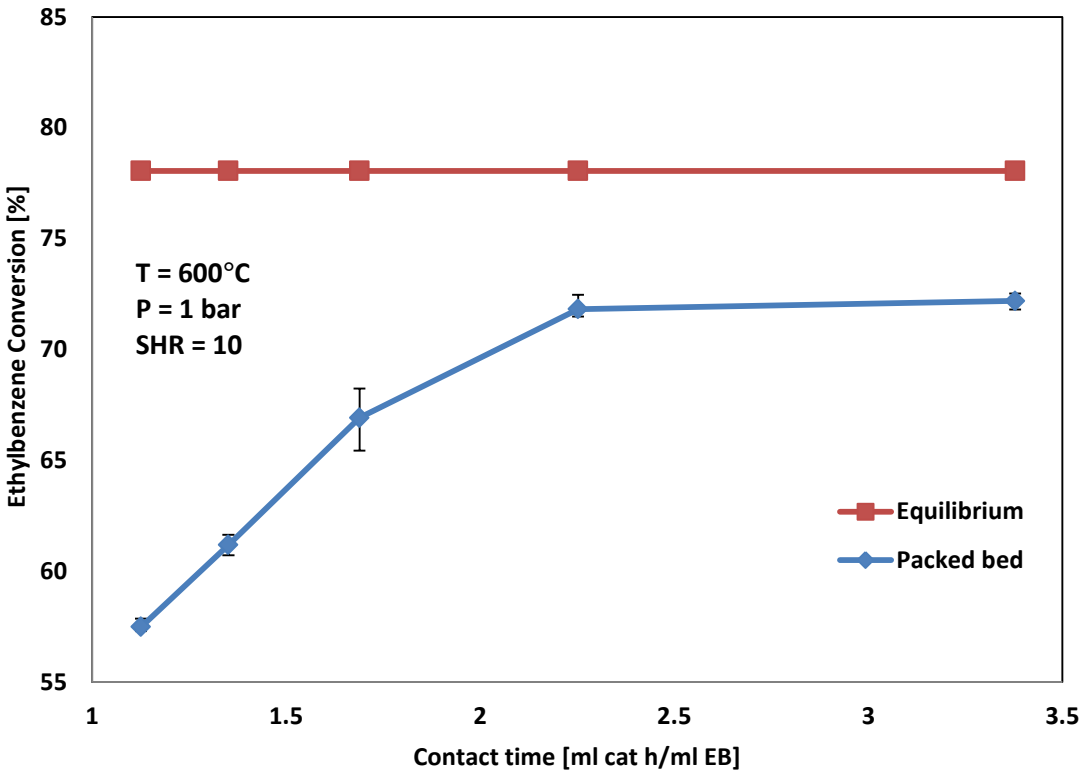

Figure 3-13 Variation of exit conversion of ethylbenzene as a function of contact time at 600°C and 1 bar pressure for crushed catalyst particles.

To ensure there were no limitations associated with internal diffusion, the Weisz Prater parameter (C_{WP}) was calculated for both catalyst sizes using the following expression obtained from Fogler [51]:

$$C_{WP} = n\varphi^2 = \frac{-r_A(obs)R^2}{D_E C_S}, \qquad (3-4)$$

where D_E is the effective diffusivity of ethylbenzene in steam, R is the pellet radius and C_S is the concentration at the pellet surface. The effective diffusivity was determined using the Fuller, Schettler and Giddings correlation [52] and was found to be about 0.09 cm^2/s for both catalyst sizes. The Weisz Prater parameter was estimated to be ~0.1 for the full size catalyst pellets at 1 bar and 625°C and ~0.05 for the catalyst particles at 1 bar and 600°C. These

values show that there are no internal diffusion limitations associated with the reaction system for both catalyst sizes.

The small size particles gave higher conversions than the pelletized form, presumably due to the combined effect of increased surface area, higher packing density and lower C_{wp}. In both cases, experimental conversions fall below the thermodynamic equilibrium levels based on the main reaction in ethylbenzene dehydrogenation (see equation (3 – 1). However, the values reported in this experimental study are higher than the conversions obtained when the effects of the side reactions were not neglected for the temperature range being considered.

In order to obtain conversions closer to equilibrium, longer contact times were employed. To achieve this, the feed flow rate of ethylbenzene was decreased since the catalyst mass was fixed by the available reactor volume. At such high contact times, the overall reaction rate is limited by external diffusion effects since most of the resistance to transfer from the bulk fluid to the surface lies in the mass transfer boundary layer surrounding the catalyst pellet. Thus, a continuous decrease of the flow rate would not lead to increased conversion due to a likely existence of external mass transfer resistance. From Figure 3-13, we see that increasing the contact time from 2.25 to 3.38 ml cat hr/ml EB only resulted in a 0.5% increase in ethylbenzene conversion.

Figure 3-14 illustrates the selectivity to styrene for the catalyst particles as a function of contact time at 600°C. Styrene selectivity decreased with increasing space time contrary to the increasing dependence of ethylbenzene conversion. This result suggests that slower side reactions become more important when the reaction mixture resides longer in the reactor.

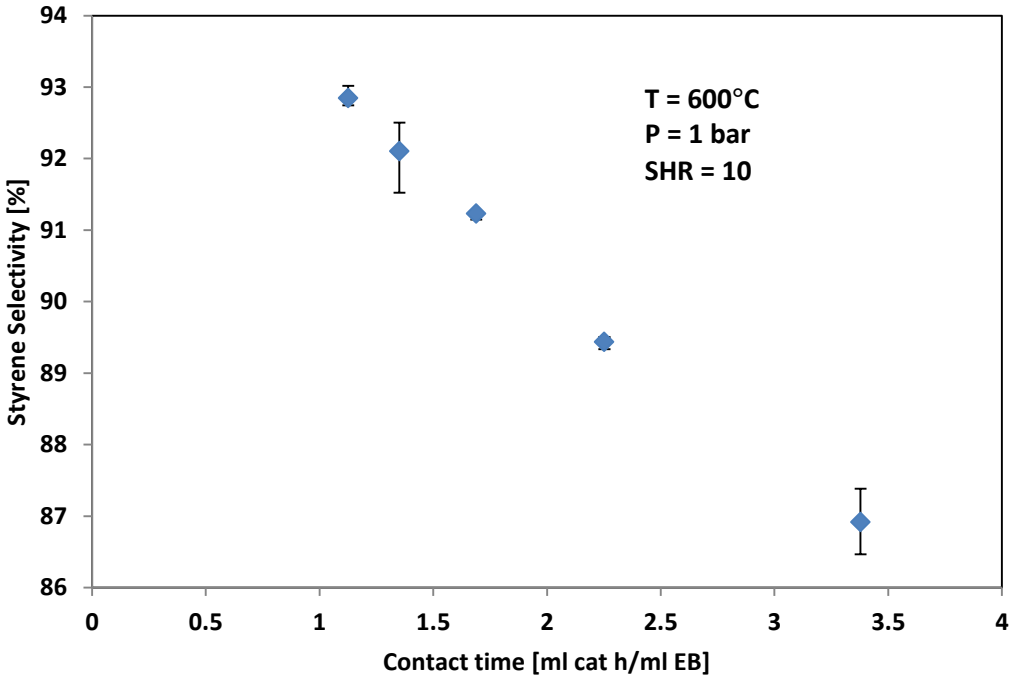

Figure 3-14 Selectivity to styrene as a function of contact time at 600°C.

Figure 3-15 shows the benzene selectivity for all the contact times considered. The benzene selectivity increased from 2% to 3% as the total ethylbenzene conversion increased from 57% to 72%. An increase in the toluene selectivity was more pronounced than benzene selectivity, as seen in Figure 3-16.Where total ethylbenzene conversion rose by a mere 0.5% between 2.25 – 3.38 ml cat h/ml EB, selectivity to toluene rose from 7.9% to 10.1%. The results obtained indicate that benzene formation is not largely influenced by the space time. The same cannot be said for toluene, whose rate of formation shows a significant enhancement with increasing space time. The existence of these undesired products is one of the main reasons why membrane reactors have been considered in order to retard the side reaction in which hydrogen is one of the reacting species.

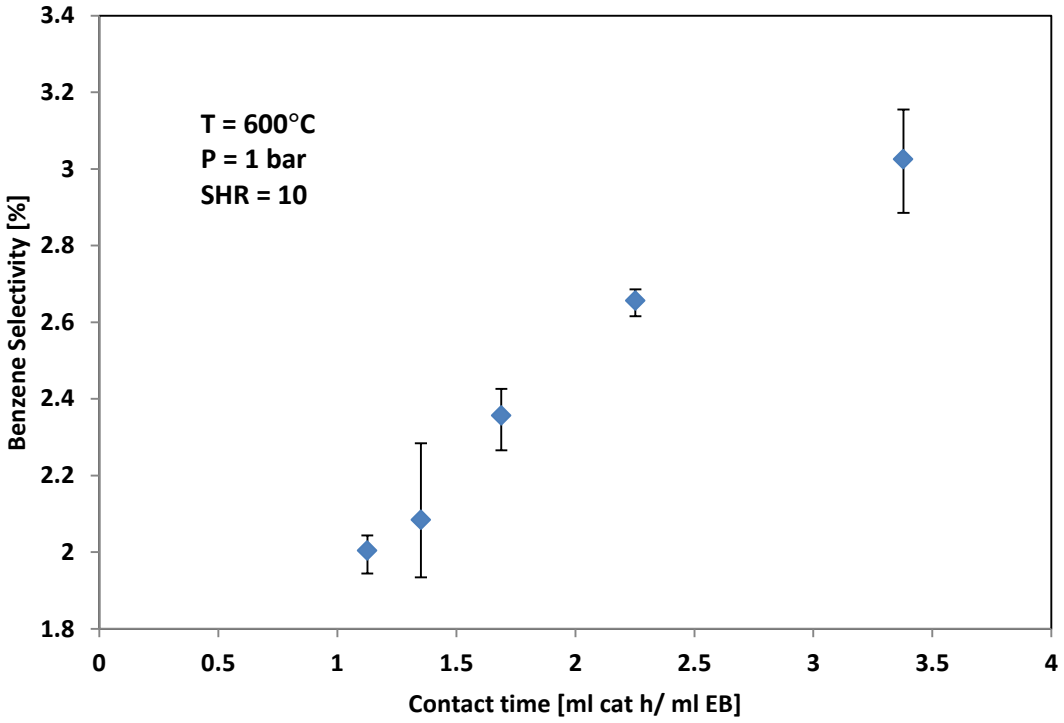

Figure 3-15 Selectivity to benzene as a function of contact time at 600°C.

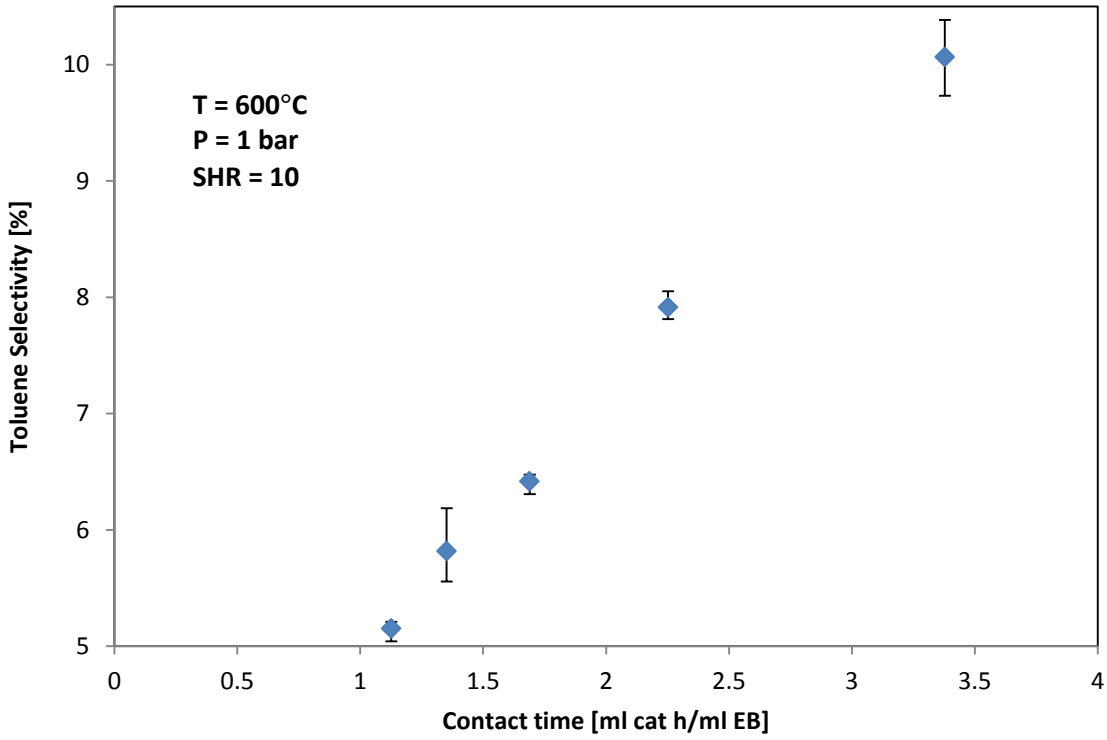

Figure 3-16 Selectivity to toluene as a function of contact time at 600°C.

3.2.3 Effect of temperature

Temperature plays an important role in the kinetics of ethylbenzene dehydrogenation. Increasing the temperature of the reaction will result in higher conversion due to faster intrinsic reaction rates. In commercial plants, increasing the reaction temperature is necessary since it offsets the decrease in catalyst activity by maintaining the required conversion [21]. Figure 3-17 illustrates the effect of temperature on the total ethylbenzene conversion at a space time of 1.69h.

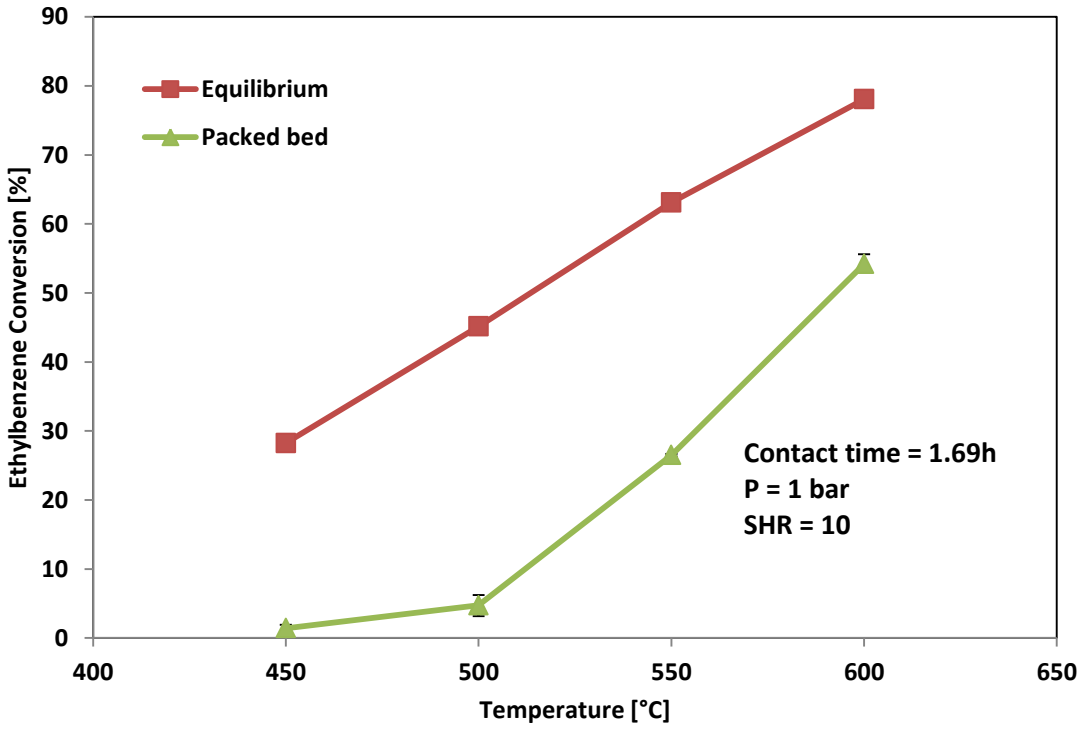

Figure 3-17 Total ethylbenzene conversion as a function of temperature at 1 bar pressure.

As expected, conversion is an increasing function of temperature. The ethylbenzene conversion ranged from as low as 1.4% at 450°C to 54.2% at 600°C. The corresponding equilibrium conversions are 28.2% and 78.1%, respectively. Since hydrogen permeation is a temperature - activated process, operating in the high temperature region would be beneficial

for the membrane reactor to achieve conversions closer to equilibrium. There is a limit, however, to how high the temperature can be raised since side reactions are more likely to occur at these higher temperatures, resulting in decreasing styrene selectivity. At temperatures higher than 600°C, a slight color discoloration was observed in the effluent stream. The color change was thought to be associated with C_7 and C_8 non-aromatics which are contained in the toluene by product during commercial production [21]. Further increase in temperature resulted in severe carbon deposition on the catalyst surface and subsequent deactivation.

3.2.4 Effect of pressure

The reaction stoichiometry for ethylbenzene dehydrogenation shows that a lower pressure will favor styrene formation from an equilibrium standpoint. Hence, most experimental studies were conducted under atmospheric and sub-atmospheric conditions. However, modeling studies predict that favorable conversions may be obtained at higher pressures. Hermann et al. [53] observed that the advantages of the membrane reactor with regards to the total ethylbenzene conversion would be small when operated at typical conditions of elevated temperature and low pressure. They reported that an increase in pressure would accelerate the reaction rate thus increasing the conversion for both fixed bed and membrane reactor configurations under conditions of inert sweep gas and permeate evacuation. Bitter [54] also claimed to have favorable results at 625°C and 4 bar pressure while employing porous ceramic membranes for ethylbenzene dehydrogenation. Figure 3-18 shows the effect of pressure on total equilibrium conversion at a temperature of 600°C.

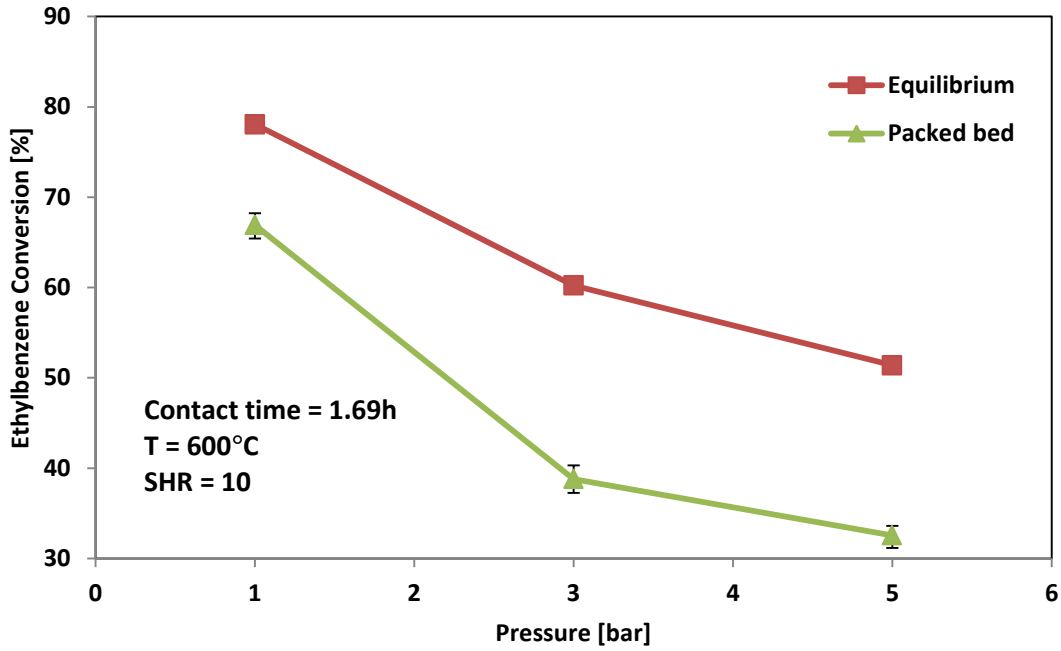

Figure 3-18 Ethylbenzene conversion as a function of pressure at 600°C.

From these data, we see that the effect of pressure is not only strong but detrimental. As pressure increases, conversion declines rapidly. Increasing the reaction pressure from near atmospheric conditions to 3bar resulted in a 23% drop in conversion. A further increase to 5 bar pressure led to a smaller drop of about 15%. Selectivity to styrene followed a similar pattern with increasing pressure dropping from 91.2% at 1 bar to 83.1% at 3bar as seen in Figure 3-19. This can be attributed to the acceleration of the reverse reaction and associated side reactions. As shown earlier in eqns. (1-8) and (1-9), toluene is not only derived from the hydroalkylation of ethylbenzene but also of styrene [21] and is favored by a pressure increase. Accordingly, the measured selectivity to toluene increased significantly.

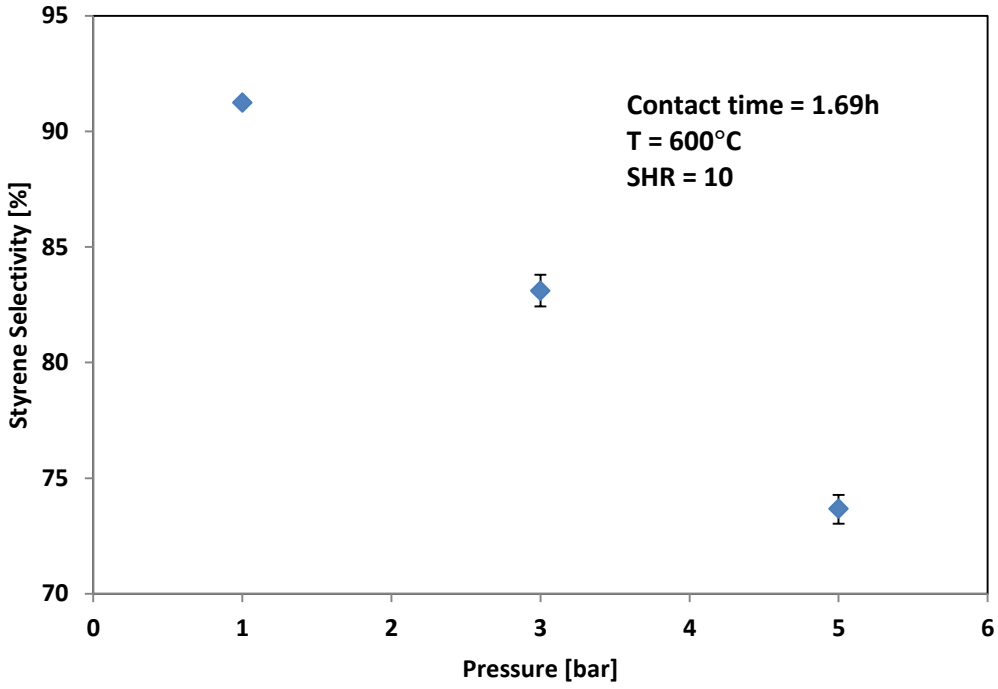

Figure 3-19 Selectivity to styrene as a function of pressure at 600°C.

A striking color change was seen in the product which intensified with increasing reaction pressure indicating the presence of other organics in the exit stream. This is not uncommon in the commercial production of styrene as slight pressure variations usually bring about a color change in the exit stream. Samples collected from the setup underwent a chemical change from colorless to light yellow and finally to dark yellow at the highest operating pressure i.e., 5 bar indicating increasing concentrations of other unidentified species. The effluent stream was also characterized by a very foul odor. This has been attributed to the presence of octadiene isomers which give off a very unpleasant smell similar to hydrogen sulfide even in small concentrations. In particular, 1, 5-cyclooctadiene (see structure below) has been reported to have a foul stench and may be responsible for the unpleasant odor noticed in the product.

C_8H_{12} or 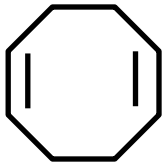

Figure 3-20 Chemical structure of 1, 5-cyclooctadiene.

3.3 Membrane reactor studies

The advantage of the membrane reactor for ethylbenzene dehydrogenation is a result of the removal of hydrogen produced during the course of the reaction. Hydrogen transport through a membrane is driven by a pressure gradient between the packed bed (retentate) side and the permeate side. Several options can be pursued to achieve this driving force; i.e., use of an inert sweep gas (such as nitrogen, helium or argon) in the retentate/permeate side, application of a pressure difference via permeate evacuation, or use of reactive sweep gas (usually oxygen) to deplete the permeated hydrogen. Experimental studies for ethylbenzene dehydrogenation in membrane reactors have focused on the application of an inert sweep gas [12, 19, 28]. In this section, we report results of membrane performance under conditions of permeate evacuation.

3.3.1 Comparison of PBR and PBMR conversions

Figure 3-21 compares the total ethylbenzene conversions for the PBR and PBMR at a space time of 1.8h and a pressure of 1 bar for temperatures ranging between 450°C – 600°C. The permeate side of the reactor was kept at 22kPa. At 500°C and below, the PBR conversion is essentially equal to the PBMR conversion. As temperature was increased and more hydrogen generated, PBR conversion slightly exceeded conversion obtained in the

PBMR. For example, at 600°C, the ethylbenzene conversion in the PBR was 8% higher than that of the PBMR.

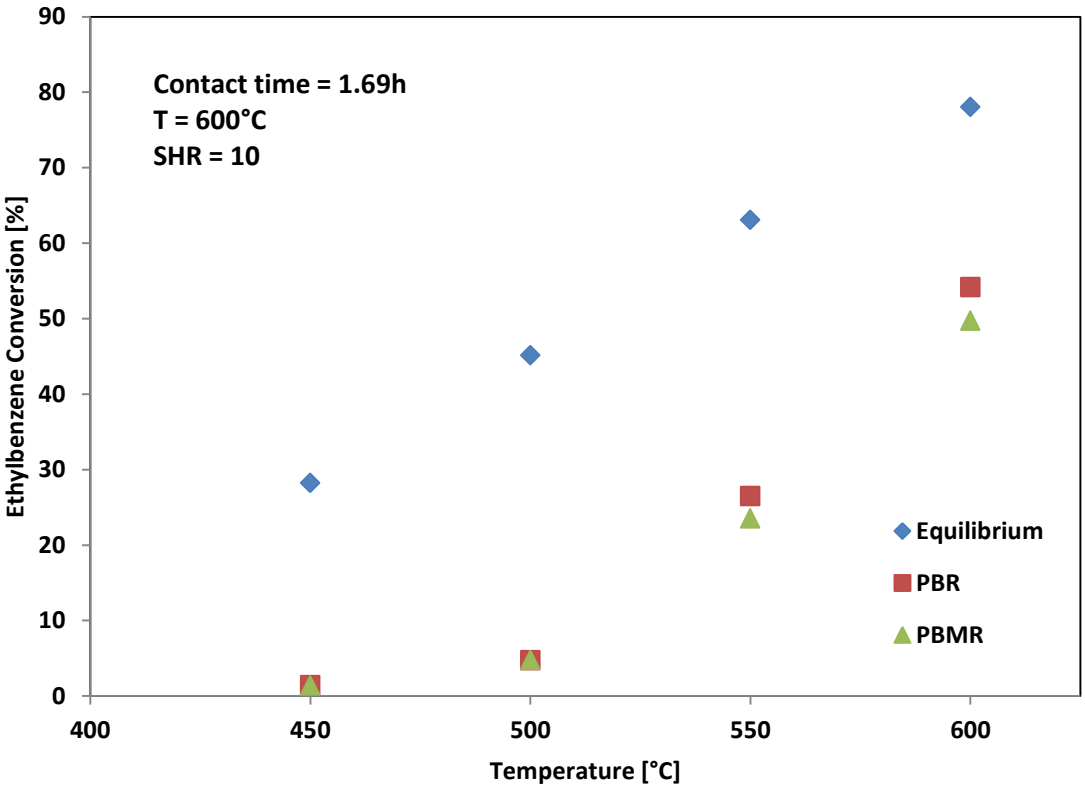

Figure 3-21 Comparison of PBR and PBMR conversions as a function of temperature for a space time of 1.8h.

This decrease in PBMR conversion is largely attributed to the fact that retentate hydrogen partial pressure is less than hydrogen partial pressure on the permeate side due to the large volume of steam present in the system. This creates a negative pressure gradient thus hydrogen generated is not recovered on the permeate side but is instead forced back into the reacting system. Sievert's expression (see eqn. (1-4)) illustrates the necessity of a positive pressure gradient to ensure the effective transport of hydrogen through the lumen side of membrane. From our observations, the backwards driving force caused hydrogen produced

during the reaction to reside longer in the reactor making it available for more unwanted side reactions.

Further decrease of permeate side pressure was not achievable due to equipment limitations. It is difficult to compare the results obtained in this work with other studies in literature given the difference in operating conditions and the catalyst used. However, it is expected that PBMR conversion would exceed that of the PBR once a positive driving force is established with the difference widening as temperature increases as established in previous studies for both ceramic and palladium coated fibers.

3.3.2 Post reaction studies – flux measurements

After the membrane reactor studies were completed, a pure hydrogen permeation test was conducted to observe and compare the transmembrane flux of the unused and used membranes. A binary test employing a 50/50 mixture of hydrogen and nitrogen gas was also used to determine the H_2/N_2 selectivity. Figures 3-22 and 3-23 show the pure hydrogen flux at 600°C before and after reactor studies.

From the plots, we see that hydrogen flux decreased by a factor of ~14 for all transmembrane pressure differences considered. For instance, at a ΔP_{H2} of 206 $Pa^{0.5}$, the flux dropped from 0.61 to 0.43 mol/m^2s. This lends more credence to the blocking of active sites for hydrogen transport by carbon deposited on the palladium surface. Other groups have reported the detrimental effects of carbon on palladium membranes for other reaction studies [37, 40, 42].

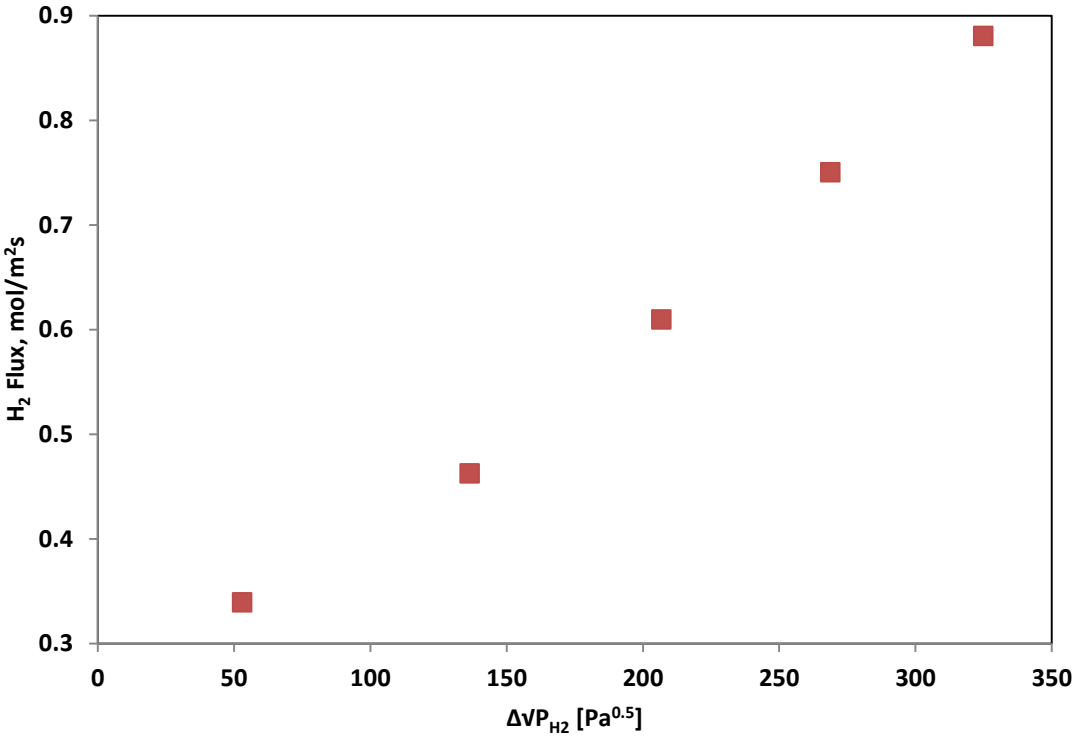

Figure 3-22 Results of permeations with H_2 at 600°C for an 11µm palladium membrane prior to reactor studies.

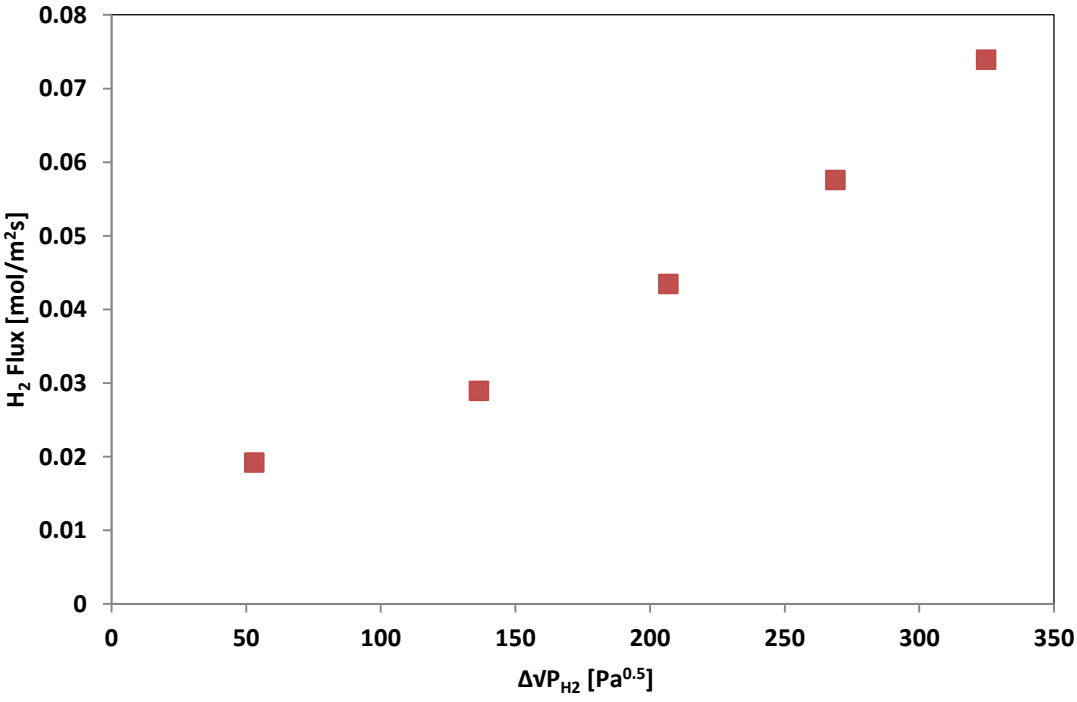

Figure 3-23 Transmembrane hydrogen flux after membrane reactor studies at 600°C.

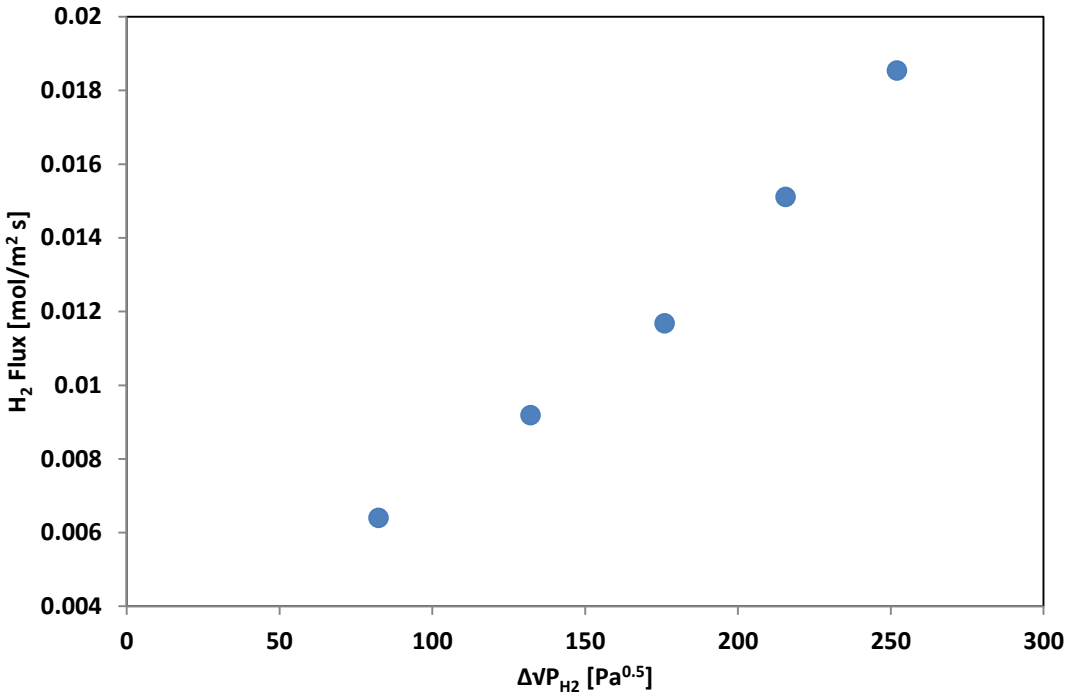

Figure 3-24 Results of binary permeation for an equimolar mixture of N_2 & H_2 after membrane reactor studies at 600°C.

Binary flux also exhibited a similar trend dropping by a factor of about 25 for the same pressure difference considered. On comparison of Figures 3-4 and 3-24, we observe that at a ΔP_{H2} of 176 $Pa^{0.5}$, binary flux fell from 0.31 to 0.012 mol/m^2s while H_2/N_2 selectivity plummeted to about 2. These results further corroborate the need for membranes that can withstand the required temperatures and gas atmospheres.

3.3.3 Post reaction studies – surface morphology

To better understand the effects the reaction species had on the membrane structure and morphology, the palladium membrane was classified by SEM analysis before and after it was used for the dehydrogenation studies. A physical comparison of the membrane before and after use was sufficient to indicate damage had been done to the palladium microstructure. As opposed to the shiny surface of the unused fiber, the palladium membrane

exposed to the reaction system was characterized by a dull, sooty appearance and noticeable swelling along its entire length.

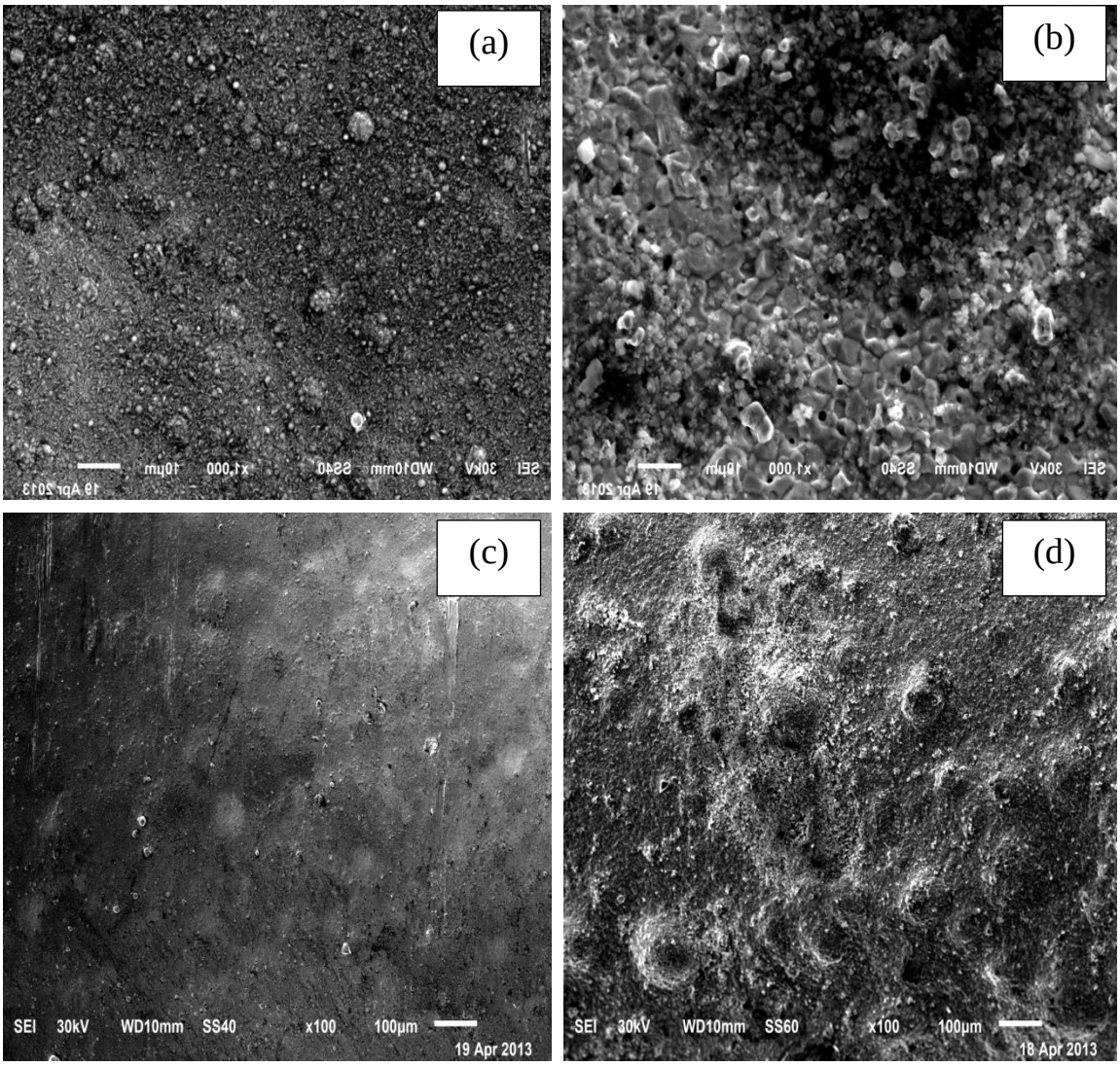

Figure 3-25: (a) and (b) are SEM images of the palladium membrane before and after ethylbenzene dehydrogenation at a resolution of 10µm. Figure (c) and (d) are images of the unused and used membrane taken at a resolution of 100µm.

Figure 3-25 shows the SEM micrographs of the surface of the palladium membrane before and after exposure to temperatures ranging from 450 – 600°C for about 168h under reaction conditions. The images shown in 3-25a and 3-25b were taken at a resolution of 10μm. The sample in 3-25a shows a large population of small grains of relatively uniform grain size with several larger circular grains interspersed among them. It can be observed that the grains are densely packed and no visible defects are seen. The image in 3-25b taken after the experiments shows a distortion of the surface microstructure. Some portions of the sample appear to have 'caved in', other parts appear flattened out and some of the grains seem to have formed clusters. There is also the development of pinholes across the entire surface which may be attributed to high temperature operation and intermetallic diffusion of components during the course of the reaction. These pinholes compromise the separation capability of the palladium membrane. The images in 3-25c and 3-25d, taken at a resolution of 100μm, clearly show the occurrence of surface deformation as a result of membrane swelling. Membrane swelling has been attributed to carbonaceous deposition under hydrogen depleted conditions [1, 2]. Pinhole formation and membrane swelling are not uncommon in membrane reactors for hydrocarbon processes as seen in studies conducted by She et al. [28] and Galuszka et al. [54]. Clearly, the stability of the palladium membrane under reaction conditions is a critical factor in the success of palladium based membrane reactors for ethylbenzene dehydrogenation.

Chapter 4

Conclusions and Recommendations for Future Work

4.1 Conclusions

In this work, composite palladium-ceramic membranes with good hydrogen permeability and permselectivity features were prepared by electroless plating for application in a commercially important, catalytic reaction, ethylbenzene dehydrogenation to styrene.

The dehydrogenation of ethylbenzene (EB) was successfully carried out in a packed bed reactor (PBR) and packed bed membrane reactor (PBMR) under identical conditions and the results compared. Two catalyst particle sizes were considered and the overall results indicate that a smaller particle size yields superior results in terms of EB conversion and styrene selectivity. The PBMR conversion was slightly lower than that of the PBR due to insufficient driving force for permeation through the membrane. This was further exacerbated by the surface adsorption of non-hydrogen species on the palladium membrane. Although higher temperatures yielded higher conversions, equilibrium values were still higher. Higher total pressure operation had a strong negative impact on the EB conversion and styrene selectivity and resulted in the formation of by-products, besides toluene and benzene, as well as other unidentified species that altered the physical appearance (color) and odor of the product. The experiments revealed that decreasing space velocities (LHSV) increased the conversion but decreased the selectivity. The implication is that one must sacrifice selectivity to obtain higher conversions and vice versa. Optimal operating conditions depend on a trade-off between temperature and LHSV.

The presence of the reactant species (H_2O, $C_6H_5CH_2CH_3$) had significant inhibition effects on the hydrogen permeation at reaction temperature (~ 600°C). The inhibition effects

increased with increasing concentrations of the non-H_2 species in the feed stream. The inhibition magnitudes were as follows: $C_6H_5CH_2CH_3 > H_2O > N_2$. This order is a reflection of the adsorption capacity on the palladium surface. A rather low concentration of ethylbenzene in the feed (5 mole percent) was sufficient to cause a hydrogen flux decrease of over 60% due to contamination by carbon deposition. Unlike water, its poisoning effects were irreversible.

The development of pinholes and membrane swelling was confirmed by SEM micrographs taken after reaction and permeation studies. The membrane deterioration and loss of the palladium's permselective capabilities was evident by flux measurements taken after the experiments. The deposition of carbon is attributed to be the main cause of membrane degradation, with time on stream.

4.2 Recommendations for Future Work

4.2.1 Membrane stability

Long term stability of membranes under reaction conditions is the major hindrance to their full scale commercialization. Nair and Harold [34] have synthesized the encapsulated membrane where a γ-Al_2O_3 was deposited on the palladium surface. These can be used as an alternative to top layer membranes and tested under reaction conditions to compare their performance to the conventional PBMR results. It is suggested that more effort be made in the synthesis of lumen-side plated membranes. Lumen-side plating reduces the exposure of the palladium surface to the reactant atmosphere and limits the risk of the thin palladium layer being 'peeled off' by abrasion with catalyst particles. Along with inside plating, the incorporation of alloys (Au, Ag) in the palladium metal would go a long way in extending the time on stream of the membrane and improve the membrane reactor performance.

4.2.2 Driving force for permeation

Most studies have employed a sweep gas for hydrogen permeation for ethylbenzene dehydrogenation [19, 28, 29]. Simulation studies [53, 56] have been performed for other methods of generating a driving force besides sweep gas but there are no experimental results to support these data. It is suggested that more research be done on the application of permeate evacuation for improvement in conversion. Practically, it is not feasible to achieve perfect vacuum but conditions close to total vacuum can be attained with a higher capacity pump. Since most commercial manufacturers of styrene already run under conditions of vacuum, this research would be very useful once the issue of membrane stability is addressed.

4.2.3 Surface studies for palladium membranes under reaction conditions

There have been no previous surface science studies reported in literature on the effects of larger hydrocarbons and aromatics on the palladium membrane surface during reaction conditions. The major reason for hydrogen flux reduction is the surface adsorption and reaction of the species with the metal. These chemisorbed species increase the energy barrier between the subsurface hydrogen states, block active sites, and interrupt hydrogen dissociation [2]. Israni et al. [33] performed a detailed study for the effect of water and other species on the hydrogen flux. Although insightful, the concentration of water considered is small compared to that used in ethylbenzene dehydrogenation and results in this study have indicated a unique trend on the effect of water on the flux. There is a great need to understand the surface chemistry on palladium and propose mechanisms that account for the interactions that occur between the reactant/product gases and the membrane. This information is crucial for extending the lifetime of the membrane under realistic conditions.

References

[1] Dittmeyer, R., Hollein, V. & Daub, K., 2001. "Membrane reactors for hydrogenation and dehydrogenation processes based on supported palladium." *Journal of Molecular Catalysis A: Chemical,* 173(1-3), pp. 135-184.

[2] Paglieri, S. & Way, J., 2002. "Innovations in Palladium Membrane Research." *Separation and Purification Methods,* 31(1), pp. 1-169.

[3] Champagnie, A., Tsotsis, T., Minet, R. & Webster, A., 1990. "A high temperature catalytic membrane reactor for ethane dehydrogenation." *Chemical Engineering Science,* 45(8), pp. 2423-2424.

[4] Elichi, K., 1995. "Palladium/ceramic membranes for selective hydrogen permeation and their application to membrane reactor." *Catalysis Today,* 25(3-4), pp. 333-337.

[5] Harold, M. P., Nair, B. & Kolios, G., 2003. "Hydrogen generation in a Pd membrane fuel processor: assessment of methanol-based reaction systems." *Chemical Engineering Science,* 58(12), pp. 2551-2571.

[6] Uemiya, S., Sato, H. A., Matsuda, T. & Kikuchi, E., 1990. "Steam reforming of methane in a hydrogen-permeable membrane reactor." *Applied Catalysis,* 67(1), pp. 223-226.

[7] Chen, Y., Wang, Y., Xu, H. & Xiong, G., 2008. "Efficient production of hydrogen from natural gas steam reforming in palladium membrane reactor." *Applied Catalysis B: Environmental,* 81(3-4), pp. 283-285.

[8] Basile, A., Criscuoli, A., Sartella, F. & Drioli, E., 1996. “Membrane reactor for water gas shift reaction.” *Gas Separation & Purification,* 10(4), pp. 243-245.

[9] Augustine, A. S., Ma, Y. H. & Kazantzis, N. K., 2011. “High pressure palladium membrane reactor for high temperature water-gas shift reaction.” *International Journal of Hydrogen Energy*, 36(9), pp. 5350-5352.

[10] Sheintuch, M. & Dessau, R. M., 1996. “Observations, modelling and optimization of yield, selectivity and activity during dehydrogenation of isobutane and propane in a Pd membrane reactor.” *Chemical Engineering Science,* 51(4), pp. 535-537.

[11] Itoh, N. & Wu, T.-H., 1997. “An adiabatic type of palladium membrane reactor for coupling endothermic and exothermic reactions.” *Journal of Membrane Science,* 124(2), pp. 213-214.

[12] Quicker, P., Hollein, V. & Dittmeyer, R., 2000. “Catalytic dehydrogenation of hydrocarbons in palladium composite membrane reactors.” *Catalysis Today,* 56(4), pp. 21-34.

[13] Basile, A., Iulianelli, T., Longo, T. & De Falco, M., 2011. “Pd-based Selective Membrane State-of-the-Art.” In: M. De Falco, G. Iaquaniello & L. Marrelli, eds. Membrane Reactors for Hydrogen Production Processes. s.l.:Springer, pp. 21-56.

[14] Nair, B. & Harold, M., 2006. “Hydrogen generation in a Pd membrane fuel processor: Productivity effects during methanol steam reforming.” *Chemical Engineering Science,* 61(19), pp. 6616-6636.

[15] Israni, S., Nair, B. & Harold, M., 2009. “Hydrogen generation and purification in a composite Pd hollow fiber membrane reactor: Experiments and modelling.” *Catalysis Today*, 139(4), pp. 299-311.

[16] Sanfilippo, D. & Rylander, N., 2009. “Hydrogenation and Dehydrogenation.” In: Ullmann's Encyclopedia of Industrial Chemistry. s.l.:Wiley-VCH, pp. 461-468.

[17] Bhasin, M., McCain, J., Vora, B. & Pujado, P., 2001. “Dehydrogenation and oxydehydrogenation of paraffins to olefins.” *Applied Catalysis A: General,* 221(1-2), p. 397.

[18] Lira, A. & Tailleur, R., 2012. “Dehydrogenation of C12 - C14 paraffins on PtCu/meso-structured Al_2O_3 catalyst for LAB production: Process simulation.” *Fuel,* Volume 97, pp. 49-50.

[19] Yu, C. & Xu, H., 2011. “An efficient palladium membrane reactor to increase the yield of styrene in ethylbenzene dehydrogenation.” *Separation and Purification Technology*, 78(2), pp. 249-252.

[20] Ozokwelu, D, 2012. *US Department of Energy.* [Online] Available at: http://www1.eere.energy.gov/office_eere/pdfs/exelus_case_study.pdf [Accessed May 2012].

[21] Chen, S., 2006. “Styrene.” In: A. Siedel, ed. Kirk Othmer Encylopedia of Chemical Technology 5th ed. New Jersey: John Wiley & Sons Inc, pp. 325-357.

[22] Addiego, W., Liu, W. & Boger, T., 2001. “Iron oxide-based honeycomb catalysts for the dehydrogenation of ethylbenzene o styrene.” *Catalysis Today,* 69(1-4), pp. 25-27.

[23] Xiang, B., Xu, H. & Li, W., 2007. “Highly Efficient Nano-sized Fe_2O_3-K_2O Catalyst for Dehydrogenation of Ethylbenzene to Styrene.” *Chinese Journal of Catalysis*, 28(10), pp. 841-843.

[24] Atanda, L., Al-Yassir, N. & Al-Khattaf, S., 2011. “Kinetic modelling of ethylbenzene dehydrogenation over hydrotalcite catalysts.” *Chemical Engineering Journal,* 171(3), pp. 1387-1388.

[25] Mimura, N. & Saito, M., 2000. “Dehydrogenation of ethylbenzene to styrene over Fe_2O_3/Al_2O_3 catalysts in the presence of carbon dioxide.” *Catalysis Today,* 55(1-2), pp. 173-174.

[26] Sun, A., Qin, Z., Chen, S. & Wang, J., 2004. “Ethylbenzene dehydrogenation inn the presence of carbon dioxide over alumia supported catalysts.” *Catalysis Today*, Volume 93-95, pp. 273-279.

[27] Zhu, X.M., Schon, M., Bartmann, U., van Veen, A.C. & Muhler, M., 2004. “The dehydrogenation of ethylbenzene to styrene over a potassium pomoted iron-oxide based catalyst: a transient kinetic study.” *Aplied Catalysis A: General,* 266(1), pp. 99-108.

[28] She, Y., Han, J. & Ma, J., 2001. “Palladium membrane reactor for the dehydrogenation of ethylbenzene to styrene.” *Catalysis Today,* 67(1-3), pp. 43-53.

[29] Elnashaie, S.S.E.H., Abdallah, B.K., Elshishini, S.S., Alkhowaiter, S., Noureldeen, M.B. & Alsoudani, T., 2001. “On the link between intrinsic catalytic reactions kinetcis and the development of catalytic processes: Catalytic dehydrogenation of ethylbenzene to styrene.” *Catalysis Today,* 64(3-4), pp. 151-162.

[30] Becker, Y., Dixon, A., Moser, W. & Ma, Y., 1993. “Modelling of ethylbenzene dehydrogenation in a catalytic membrane reactor.” *Journal of Membrane Science* , 77(2-3), pp. 233-244.

[31] Yang, W.-S., Wu, J.-C. & Lin, L.-W., 1995. “Application of membrane reactor for dehydrogenation of ethylbenzene.” *Catalysis Today*, 25(3-4), pp. 315-319.

[32] Kong, C., Lu, J., Yang, J. & Wang, J., 2007. “Catalytic dehydrogenation of ethylbenzene to styrene in a zeolite silicalite-1 membrane reactor.” *Journal of Membrane Science,* 306(1-2), pp. 29-30.

[33] Israni, S. & Harold, M., 2010. “Methanol Steam Reforming in Pd-Ag Membrane Reactors: Effects of Reaction System Species on Transmembrane Hydrogen Flux.” *Industrial Engineering Chemical Research,* Volume 49, pp. 10242-10250.

[34] Nair, B. & Harold, M., 2007. “Pd encapsulated and nanopore hollow fiber membranes: Synthesis and permeation studies.” *Journal of Membrane Science,* Volume 290, pp. 182-195.

[35] Collins, J. & Way, J., 1993. “Preparation and Characterization of a Composite Palladium-Ceramic Membrane.” *Industrial Engineering Chemical Research,* Volume 32, pp. 3006-3013.

[36] Nair, B., Choi, J. & Harold, M., 2007. “Electroless plating and permeation features of Pd and Pd/Ag hollow fiber composite membranes.” *Journal of Membrane Science,* 288(1-2), pp. 67-84.

[37] Peters, T., Stange, M., Klette, H. & Bredesen, R., 2008. “High pressure performance of thin Pd-23%Ag/stainless steel composite membranes in water gas shift gas

mixtures; influence of dilution, mass transfer and surface effects on the hydrogen flux." *Journal of Membrane Science,* 316(1-2), pp. 119-127.

[38] Nair, B. & Harold, M., 2008. "Experiments and modeling of transport in composite Pd and Pd/Ag coated alumina hollow fibers." *Journal of Membrane Science,* Volume 311, pp. 53-67.

[39] Gielens, F.C., Knibbeler, R.J.J., Duysinx, P.F.J., Tong, H.D., Vorstman, M.A.G. & Keurentjes, J.T.F., 2006. "Influence of steam and carbon dioxide on the hydrogen flux through thin Pd/Ag and Pd membranes." *Journal of Membrane Science,* 279(1-2), pp. 176-185.

[40] Catalano, J., Baschetti, M. & Sarti, G., 2011. "Influence of water vapor on hydrogen permeation through 2.5um Pd-Ag membranes." *International Journal of Hydrogen Energy,* 36(14), pp. 8658-8673.

[41] Li, A., Liang, W. & Hughes, R., 2000. "The effect of carbon monoxide and steam on the hydrogen permeability of a Pd/stainless steel membrane." *Journal of Membrane Science,* 165(1), pp. 135-141.

[42] Hou, K. & Hughes, R., 2002. "The effect of external mass transfer, competitive adsorption and coking on hydrogen permeation through thin Pd/Ag membranes." *Journal of Membrane Science,* Volume 206, pp. 119-130.

[43] Galluci, F., Chiaravalloti, F., Tosti, S., Drioli, E. & Basile, A., 2007. "The effect of mixture gas on hydrogen permeation through a palladium membrane: Experimental study and theoretical approach." *International Journal of Hydrogen Energy,* Volume 32, pp. 1837-1845.

[44] Unemoto, A., Kaimai, A., Sato, K., Otake, T., Yashiro, K., Mizusaki, J., Kawada, T., Tsuneki, T., Shirasaki, Y. & Yasuda, I., 2007. "Surface reaction of hydrogen on palladium alloy membrane under co-existence of H_2O, CO, CO_2, CH_4." *International Journal of Hydrogen Energy*, Volume 32, pp. 4023-4029.

[45] Yoshida, H., Konishi, Y. & Naruse, Y., 1983. "Effects of impurities on hydrogen permeability through palladium alloy membraes at comparatively high pressures and temperatures." *Journal of the Less Common Metals*, 89(2), pp. 429-436.

[46] Itoh, N., Xu, W.-C. & Haraya, K., 1992. "Basic experimental study on palladium membrane reactors." *Journal of Membrane Science*, 66(2-3), pp. 149-155.

[47] Stachurski, J. & Frackieicz, A., 1985. "A new phase in the Pd-C system formed during the ctatlytic hydrogenation of acetylene." *Journal of the Less Comon Metals*, 108(2), pp. 249-256.

[48] Ali, J., Newson, E. & Rippin, D., 1994. "Deactivation and regeneration of Pd-Ag membranes for dehydrogenation reactions." *Journal of Membrane Science*, 89(1-2), pp. 171-184.

[49] Jung, S., Kusakabe, K., Morooka, S. & Kim, S.-D., 2000. "Effects of co-existing hydrocarbons on hydrogen permeation through a palladium membrane." *Journal of Membrane Science* , 170(1), pp. 53-60.

[50] Sato, K., Nishioka, M., Higashi, H., Inoue, T., Hasegawa, Y., Wakui, Y., Toshishige, M., Hamakawa, S., 2012. "Influence of CO_2 and H_2O on the separation of hydrogen over two types of Pd membranes: Thin metal membrane and pore-filling type membrane." *Journal of Membrane Science,* Volume 415-416, pp. 85-92.

[51] Fogler, H., 1986. Elements of Chemical Reaction Engineering. New Jersey: Prentice Hall

[52] Fuller, E., Schettler, P. & Giddings, C., 1966. "A new method for prediction of binary gas phase diffusion coefficients". *Industrial and Engineering Chemistry*, Volume 58, pp. 18-27.

[53] Hermann, C., Quicker, P. & Dittmeyer, R., 1997. "Mathematical simulation of catalytic dehydrogenation of ethylbenzene to styrene in a composite palladium membrane reactor." *Journal of Membrane Science*, 136(1-2), pp. 161-172.

[54] Bitter, J., 1988. *Process and apparatus for the dehydrogenation of organic compounds.* s.l. Patent No. GB2201159.

[55] Galuszka, J., Pandey, R. & Ahmed, S., 1998. "Methane conversion to syngas in a palladium membrane reactor." *Catalysis Today*, 46 (2-3), pp. 83-89

[56] Dittmeyer, R., Hollein, V., Quicker, P., Emig, G., Hausinger, G. & Schmidt, F., 1995. "Factors Controlling the Performance of Catalytic Dehydrogenation of Ethylbenzene in Palladium Composite Membrane Reactors." *Chemical Engineering Science*, 54(10), pp. 1431-1439.